DEVELOPMENT AND STUDY OF HYDROGEL-BASED FLEXIBLE MICROVALVES FOR LAB-ON-A-CHIP SYSTEMS

by

Ang Li

B.Sc., Pennsylvania State University

Thesis submitted in partial fulfillment

of the requirements for the degree of

Master of Applied Science

In the

School of Engineering Science

Faculty of Applied Science

SIMON FRASER UNIVERSITY

Spring 2012

APPROVAL

Name: **Ang Li**

Degree: **Master of Applied Science**

Title of Thesis : **Development and study of the hydrogel-based flexible microvalves for lab-on-a-chip applications**

Examining Committee:

Chair: **Dr. Stephan Robinovitch**
Professor
School of Engineering Science , Simon Fraser University

Dr. Bonnie Gray, P. Eng
Senior Supervisor
Associate Professor
School of Engineering Science, Simon Fraser University

Dr. Ash Parameswaran, P. Eng
Supervisor
Professor
School of Engineering Science, Simon Fraser University

Dr. Andrew H.Rawicz, P. Eng
Internal Examiner
Professor,
School of Engineering Science, Simon Fraser University

Date Defended/Approved: April 03, 2012

ABSTRACT

Stimuli-responsive hydrogels such as poly(N-isopropylacrylamdie) (PNIPAAm) are excellent materials for microvalves due to their biocompatibility and high energy conversion efficiency. Hydrogel-based microvalves are simple to fabricate and operate compared to other actuation schemes. While many other hydrogel-based valves have been developed by other researchers, the valves presented here differ in the use of polymers as the basis for all microvalve components for increased flexibility. This work presents the design, fabrication and characterization of a hydrogel-based plug-type microvalve and a hydrogel-based microvalve diaphragm actuator. The two designs for the valve actuation scheme are presented: 1) a microvalve diaphragm actuator; and 2) a hydrogel plug actuator. The diaphragm actuator can be fabricated employing traditional soft lithography processes for fabrication of all components, including the nanocomposite polymer (NCP) heater element, the hydrogel reservoir, and the deflecting polymer membrane. The actuation is provided by the hydrogel-actuated diaphragm deflection, with the application of heat opening a normally closed microvalve via de-swelling. The hydrogel plug element can be patterned and inserted into the structure as a fluidic control component within a microfluidic channel. The swelling and shrinking of the hydrogel plug in the microchannel results in closing and opening of the valve within 20 seconds.

ACKNOWLEDGEMENT

First and foremost, I would like to thank my senior supervisor, Dr. Bonnie Gray, without her, I would never get to this far. I am grateful for her patience, support and guidance. It wasn't a easy transition in the beginning for me. It took me a while to adjust to new environment, new school especially transition from undergraduate studies to graduate studies, but Bonnie has never lost faith in me, continue to encourage me to strive more. I hope I lived up to Bonnie' s expectation.

I would like to thank all the member within the Microinstrumentation Laboratory. Thanks for all your support, guidance and encouragement. I would also like to especially thank Dr. Paul Li, Jonathan Lee in chemistry department. Thanks for all the help with the chemistry experiment in order for this project to be successful. I also want to thank Dr. Karen Cheung(UBC), Dr.Boris Stoeber(UBC) for their insightful discussion about hydrogel. I would also like to thank the members of SFU Surrey Mechatronics program for use of the Laser cutter. I also like to thank Dr. Ash Parameswaran and Dr. Andrew Rawicz for serving on my committee. Finally, I would like thank the Canadian National Engineering and Science Research Council(NSERC) and Canadian Foundation for Innovation(CFI) for project funding.

Dedication

To my parents.

Table of Contents

LIST OF FIGURES

List of Tables

LIST OF EQUATIONS

LIST OF ACRONYMNS

The following is a list of acronyms referred to in this thesis.

C-NCP	Conductive Nanocomposite Polymer
LCST	Lower critical solution temperature
PNIPAAm	Poly-(N-isopropylacrylamide)
PCR	Polymerase Chain Reaction
PDMS	Polydimethylsiloxane
PEB	Post-Exposure Bake
PR	Photoresist
PTT	Phase Transition Temperature
IPA	Isopropyl alcohol
RIE	Reactive Ion Etching
DI	De-Ionized
PMMA	Polymethylmethacrylate
SPHs	Superporous Hydrogel
MEMS	Microelectromechanical Systems
FESEM	Field Emission Scanning Electron Microscope
µTAS	Micro Total Analysis Systems
FSI	Fluidic Structure Interaction

1 Introduction

Micro-Total Analysis systems (μTAS) and labs-on-a-chip (LOC) are integrated technologies that employ passive and active microfluidic devices to transport, manipulate, and analyze very small amounts of fluid for a variety of medical, environmental, and industrial applications. Such microfluidic systems consist of various components, including micromixers, microchannels, microvalves, pumps, and interconnect structures that are combined for a variety of microfluidics-based LOC and μTAS applications[1-2]. It can be argued that microvalve is one of the most important, and certainly one of the best studied, microfluidic components[3]. The microvalve is a component to precisely regulate the flow in many microfluidic systems.

Many traditional microvalves successfully utilize magnetic, electrostatic, mechanical, pneumatic, or piezoelectric actuation schemes[5,6,7,8]. However, many of these valves have been based in traditional microelectromechanical system (MEMS) materials such as silicon, with actuation schemes that are difficult to adapt to polymer-based microsystems. Polymer microsystems continue to increase in popularity, especially for application in microfluidic LOC and μTAS[9], and there is a similar demand for microfluidic valves compatible with or completely fabricated in polymers. Microvalve technology for mechanically flexible polymer microsystems remains a largely unexplored area. However, not only would flexible polymer microvalves be generally applicable to polymer microsystems, but they would further allow the exciting fields of microfluidic LOC and μTAS to be applied to flexible wearable and implantable microsystems[10] or to those located in flexible packaging such as contact lenses[11]

Hydrogels are excellent materials for polymer-based microvalve actuation due to their biocompatibility and energy conversion efficiency; their ability to deflect polymer

membranes, which can be employed as microvalve actuators; and their ability to expand and contract under external stimulus. Hydrogels have been investigated extensively in biomedical and microfluidic applications due to their ease of actuation: large degrees of swelling/shrinking can be realized through changes in temperature, pH levels, electromagnetic fields, or ionic strengths. The porous nature of hydrogel polymers has been utilized in other applications such as dialysis, gel electrophoresis, sample separation, and tissue engineering. Hydrogel-based microvalves have many advantages, such as simple fabrication and operation, good sealing, and high pressure for fluid. Several research groups have developed and applied stimuli-responsive hydrogels in microvalve designs[12,13,14,15] while employing them on a nonflexible substrate[16,17,18]. The microvalve presented in this thesis is different because the all parts of the microvalve were fabricated in flexible polymers.

Two designs for the valve actuator are discussed: (1) A microvalve membrane actuator and (2) a gel plug actuator. The diaphragm actuators can be fabricated using the standard soft lithography method. The gel plug valve can be fabricated by patterning the hydrogel into simple plugs and precisely inserting as fluidic control elements into a PDMS channel. Pressure and flow simulation results support the validity of the theoretical value of the hydrogel plug design.

Chapter Outline

Chapter 2 summarizes the background for the hydrogel-based microfludic devices. The design of the hydrogel-based microactuator and microvalve are discussed in Chapter 3. Chapter 4 details the fabrication of the microvalve including hydrogel synthesis and device fabrication. Chapter 5 discusses the testing and fluidic control results of the hydrogel-based microvalve. Chapter 6 discusses the simulation of the hydrogel-based microvalve both with hydrogel actuator design and hydrogel plug design. Potential applications are discussed in Chapter 7 and finally the conclusion and future work in Chapter 8.

2 Background

2.1 Overview: Stimuli-responsive Hydrogel

Hydrogels are a class of cross-linked polymers that can hold large volumes of water and have been investigated extensively in biomedical and microfluidic applications due to their degree of controllable swelling/shrinking. The effect of the swelling and de-swelling of the hydrogels in reaction to external stimulus (e.g., changes in temperature, pH levels, electromagnetic fields, or ionic strengths) has often been utilized to construct microvalves or micropumps in microfluidic systems[19].

The hydrogel PNIPAAm is a thermo-sensitive polymer that exhibits reversible phase transition from a swollen hydrated state to a dehydrated state. This reversible phase transition can also be described theoretically as gas-liquid(hydrated to dehydrated state) phase transition[20]. Figure 2-1 illustrates the hydrogel used for fabricating the microactuator, showing the transition from transparent (swollen) to milk white (shrunken) during the change from room temperature to phase transition temperature.

When the hydrogel is immersed in a solvent(e.g water), the free energy of mixing in the form of osmotic pressure causes the solvent to diffuse into the hydrogel's body. The solvent absorption leads to the expansion of the network(swelling). The solvent absorption will not stop until the complete dissolution of the polymer occur. This swelling process is due to the elastic stretching of the polymer chain between the crosslinking points[49].

The degree of swelling of PNIPAAm in aqueous solution has been extensively investigated by other researchers. They have shown that PNIPAAm hydrogel is a feasible material for use in microvalve fabrication in microfluidic systems[21] Moreover, as reported by previous researchers[22], NIPAAM hydrogel-based microvalves are relatively simple to fabricate and operate compared to other actuation schemes.

In recent years, there has been a growing interest in developing microfluidic systems for chemical and biological applications. Typically, a microfluidic device consists of pumps, conduits, connectors, valves, and pumps. PNIPAAm is a perfect example of material suitable for application in microfluidics, including hydrogel valves, hydrodynamic transistors, pumps and liquid sensors, and actuators in microfluidic and

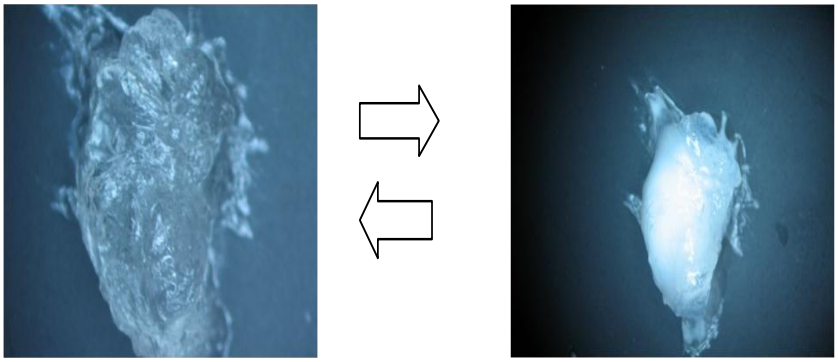

Figure 2-1 PNIPAAm hydrogel showing temperature transition : (a) when it is below 32ºC, the hydrogel swells (transparent); (b) when the hydrogel is higher than 34 ºC, the hydrogel shrinks (milk white).

LOC application.

The composition of the fluid can influence the swelling of the hydrogel. For example, it has been reported that most hydrogels swell faster in buffered solutions[48]. The pH of the fluid can cause a concentration difference of ions between the inside and outside of the gel, so fluids with different pH have different swelling characteristics. Some ions can diffuse into the gel while other ions diffuse out of the gel[48] . The osmotic pressure also plays an important role in terms of swelling where osmotic pressure inside the gel is higher than the outside of the gel when swelling. Thus, it should be noted that for all experiments in this thesis, simple water is used. However, if a

buffered solution such as that used for many biochemical experiments, or a sample with a non-neutral pH were employed instead, then the experimental results of swelling times and degree may vary somewhat from those found in this thesis work.

Microvalve actuators are the simplest hydrogel-based components in microfluidic systems. The microvalve actuators or plug structures can be placed in the microchannel or chamber. As illustrated in table 2-1, hydrogel-based microvalves have high pressure resistance, which prevents leakage. Wang et al. [23] used non-flexible microvalves in a polymerase chain reaction (PCR) chip, and Ritchter et al.'s [24] valves were commercialized as a single component.

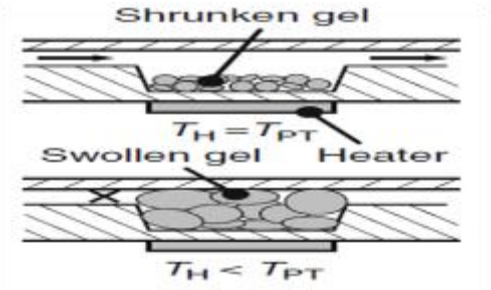

Figure 2-2 Hydrogel-based microvalve principle according to [24]

The PNIPAAm hydrogel exhibits LCST behavior at temperature of around 34°C. The thermally sensitive PNIPAAm swells at room temperature and shrinks/opens the valve when heated above the volume phase transition temperature. Figure 2-2 illustrates the basic working principle of the hydrogel-based microvalves. Table 2-1 illustrate the different kinds of hydrogel-based microvalves[24-28] developed by previous researchers.

Table 2-1 Summary of Non-flexible Hydrogel-based microvalves [24,25,26,27,28]

Authors	Valve Volume in mm^3	Pressure resistance in kPa	Time in seconds Opening/closing time
Richter 2001[24]	0.05	840	0.3/1
Yu 2003([25])	16	350	3–4/3–4
Luo 2003([26])	20	18000	1/2
Sugiura 2007[27]	0.02	0.3	18–30/ n.s.
Chen 2008[28]	n.s.	9300	4/6.2

2.2 Hydrogel-based Pumps

Hydrogel pumps can be subcategorized as autonomous hydrogel pumps and stimuli-responsive micro-pumps.

Hydrogel-based pumps are described as disposable, portable, and inexpensive devices that perform liquid pumping autonomously, without any external power sources. The insulin pump reported in [29] was developed for the treatment of the diabetes mellitus patients. The hydrogel-based pump utilizes a four task sequence to realize its function.

The task-actuating sequence is illustrated in Figure 2-3(a). The pump is initially activated by switching on the swelling agent supply. A spring generates a permanent hydrostatic pressure within the swelling agent reservoir and provides a position-independent swelling agent supply. The hydrogel swells and stretches a foil. The actuator then displaces a friction piston. The length of the displacement between

the pump initialization and start of the drug release can be changed by adjusting the relevant screw. The gel actuator presses the drug ampoule to the opener to open the sterile ampoule after period of time. Finally, the hydrogel actuator displaces the ampoule content, and the pump releases the drug [29].

The pump shown in Figure 2-3 (b) can be initialized using a droplet of water. Disposable autonomous pumps do not require hydrogels with volume phase transition behavior. The strong swelling super-absorbers can be used, which are usually more powerful than stimuli-responsive gels. The performance of the hydrogel-based pumps is defined by the size of the actuator and the material. The actuator used in [29] provides a maximal pressure of 200kPa and is designed to release 500µL insulin within 2 hours.

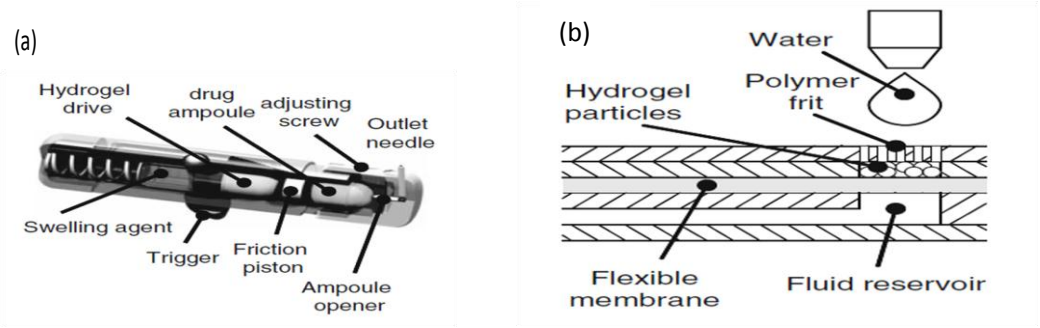

Figure 2-3 Hydrogel-Based Micropumps:
(a) Medical pump with time-delay and ampoule opener functions as in [29]
(b) Portable water-activated pump as in [30]

2.3 Other hydrogel-based devices

Other hydrogel-based devices include hydrodynamic transistors and

hydrogel-based sensors. The hydrodynamic transistors can be divided into two categories based on function as the gel actuator (depicted in Figure 2-4): The first type uses direct acting hydrogel components; the second type of hydrogel transistor employs the hydrogel acting as a servo drive.

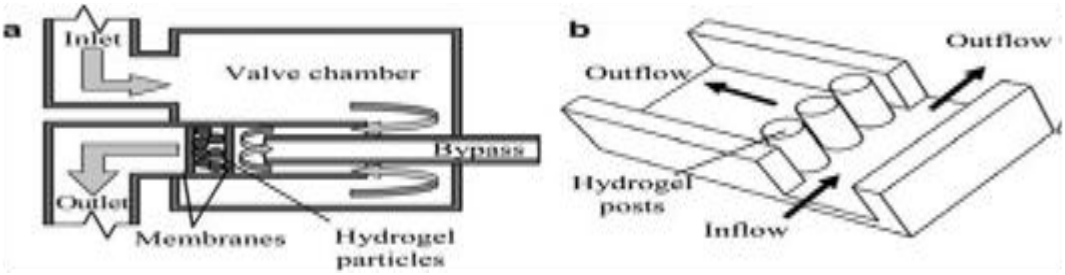

Figure 2-4 Hydrogel-based Transistor: (a) with hydrogel particles according to [31] and (b) with photopolymerised hydrogel posts according to [32]

As illustrated in Figure 2-4(b), the hydrogel shrinks when the temperature of the thermoreponsive hydrogel is above 32C; when it is below 32°C, the gel absorbs water and swells.

For sensing applications, stimuli-responsive hydrogels have attracted attention in the extensively developing field of polymers with sensors functions. The hydrogel is sensitive to different physical parameters, such as temperature, pH levels, electromagnetic fields, or concentration of ionic compounds, which increases their value in a variety of applications as chemical or biosensors. Stimuli-responsive hydrogels sensors can be applied to the fields of biotechnology, biomedical instrumentation, in the food industry, in water treatment, and so forth. Using a functionalized hydrogel coating in sensors allows them to detect, transmit, and record information regarding the

concentration change or the presence of specific analytes by producing a signal proportional to the concentration of the target analyte. These sensors can be embedded in a microfluidic system for real-time monitoring of organic and inorganic contaminants.

Stimuli-responsive hydrogels significantly change in volume in response to small changes of certain physical stimuli or parameter. Stimuli-responsive hydrogels are capable of converting chemical energy into mechanical energy. This makes them suitable as the sensitive material for sensing a chemical or biological analyte. Such sensors can have a simple and straightforward designs with high sensitivity and selectivity.

The operating principle of a hydrogel-based sensor is illustrated in Figure 2-5. The aqueous solution is injected from the inlet of the microchannel and induces the swelling or shrinking processes of the hydrogel inside the microchannel. The bending of the plate causes a stress difference inside the plates, which translates to the output voltage change ΔU_{out} of the resistor.

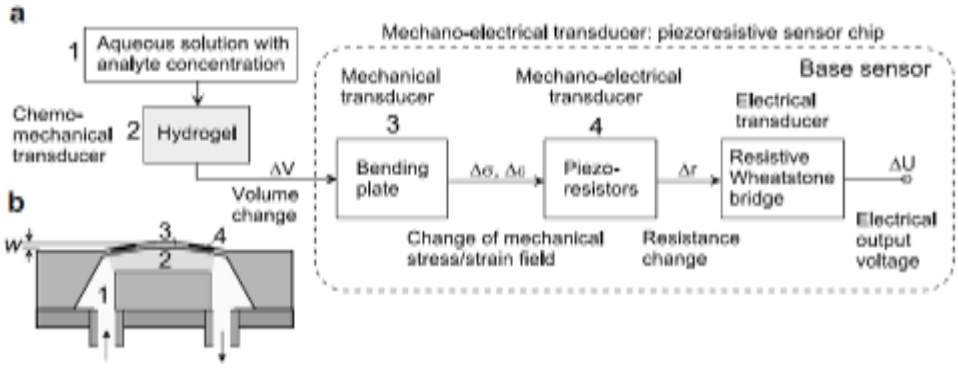

Figure 2-5 Hydrogel-based Sensor Design: 1. Bending plate. 2. MEMS transducers 3. Swellable hydrogel 4. Silicon Substrate 5. Socket 6. Inlet 7. Interconnect 8. Analyte solution 9. Si Chip

3 Design of the Hydrogel-Based Microvalve

Even though many of these devices are successful, very little research has been conducted on methods that introduce hydrogels into mechanically flexible devices. The design, fabrication, and testing of such flexible hydrogel-based microvalves devices will be discussed in the next three chapters.

A method has been developed to produce hydrogel-based flexible devices. The microvalve actuator and microvalves show promise as useful, hydrogel-based, flexible micro devices. In the following chapter, two such designs will be thoroughly discussed: (1) the microvalve diaphgram actuators and (2) the plug valve actuator

3.1 Hydrogel-based Actuator design

Figure 3-1 depicts the basic structure of the proposed thermoresponsive microvalve actuator. Two side-by-side actuators can be used to open and close two microchannels that would be directly bonded on top of the polydimethylsiloxane (PDMS) membranes after oxygen plasma etching. The actuator is composed of a reservoir containing the thermo-sensitive hydrogel PNIPAAm covered by a ~100 μm-thick PDMS membrane that acts as a deflecting diaphragm into the microchannels. Each reservoir chamber measures 3 cm in width and length and is 1 cm thick and contains thermally responsive hydrogel. The actuator also consists of a flexible, tungsten-based C-NCP heater that can provide the temperature transition for the thermoresponsive hydrogel. The hydrogel shrinks (deswells) when the temperature rises above 32 ºC; when it drops below 32 ºC, the gel absorbs water and swells. Thus, a valve employing this actuator would normally be closed and would open when powered (heated). The entire microvalve would have great mechanical flexibility compared to other valves, and the entire package could be expected to conform to curved surfaces. It is also expected that, as shown here and as demonstrated in our fabricated micro-actuators, arrays of such

microvalves could be created using batch fabrication.

As illustrated in Figures 3-1 and 3-2, each microactuator consists of (1) a W-PDMS or other nanoparticle-doped C-NCP flexible heater; (2) a flexible PDMS diaphragm; and (3) a reservoir of the thermally responsive hydrogel PNIPAAM. The

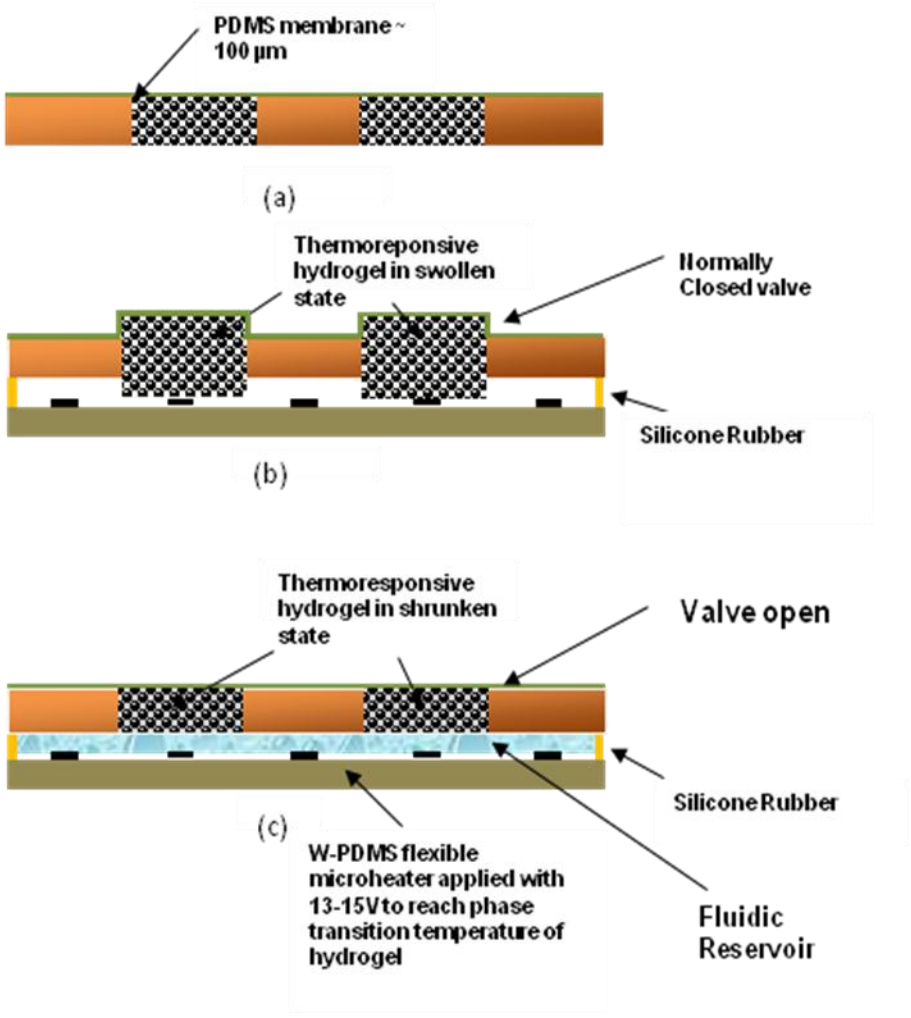

Figure 3-1 Overall design of polymer mechanically flexible microvalve actuators using thermally responsive hydrogel. Two side-by-side microvalve actuators are shown.

reservoir was situated between the microheater and PDMS membrane. It could also be situated on top of the microchannel depending on application. Microchannels could easily be added via bonding on top of the PDMS surrounding the diaphragm so that the diaphragm normally fills (and closes) the channel. The microfluidic channel could be fabricated by micromolding of poly-dimethylsiloxane (PDMS, sylgard 184) against an SU-8 or PMMA micromold.

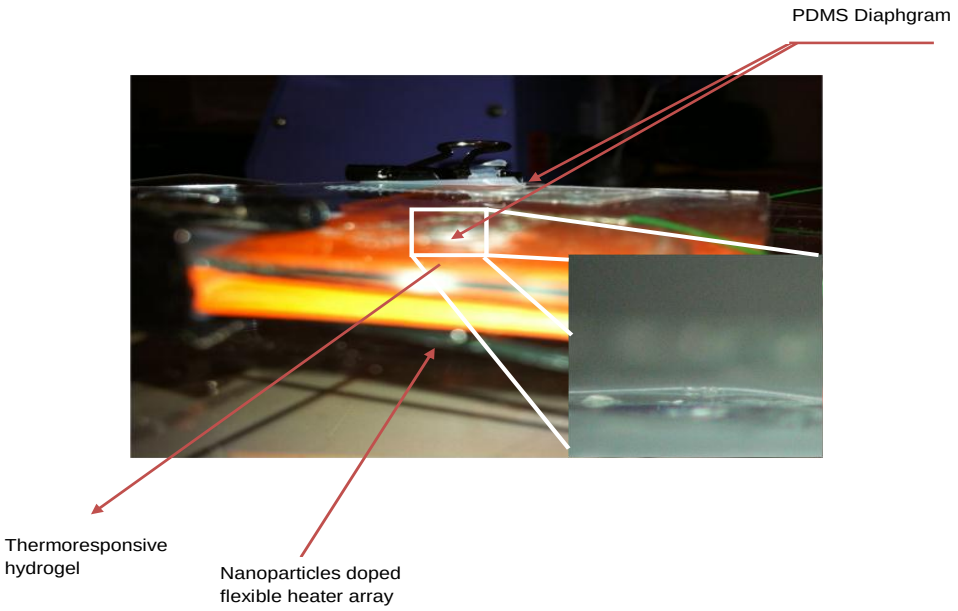

Figure 3-2 The overall setup of the fabricated hydrogel-based microactuator

3.2 Hydrogel Plug design

For the second design, 500 µm-square micropatterned hydrogel plug structures were used as fluidic control components. Two microvalve experiments were developed employing micropatterning of the PNIPAAm hydrogel. In the first case, the PNIPAAm hydrogel was confined in polyethylene tubing of 0.58mm inner diameter (purchased from Intramedic). In the second case, the hydrogel was inserted into a PDMS channel of 500µm x 500µm x 5cm, as illustrated in figure 3-5, with anchors on either side to prevent the plug from moving down the length of the channel under flow. The microchannel was fabricated using conventional soft lithography processing. Each of these designs was then affixed to the flexible heaters. The hydrogel plug inside the PDMS channel was actuated externally by the flexible heaters element. The role of the temperature-responsive hydrogel is to control the fluidic flow by opening and closing the tubing or microchannel, thus acting as a normally-closed, in-plane valve.

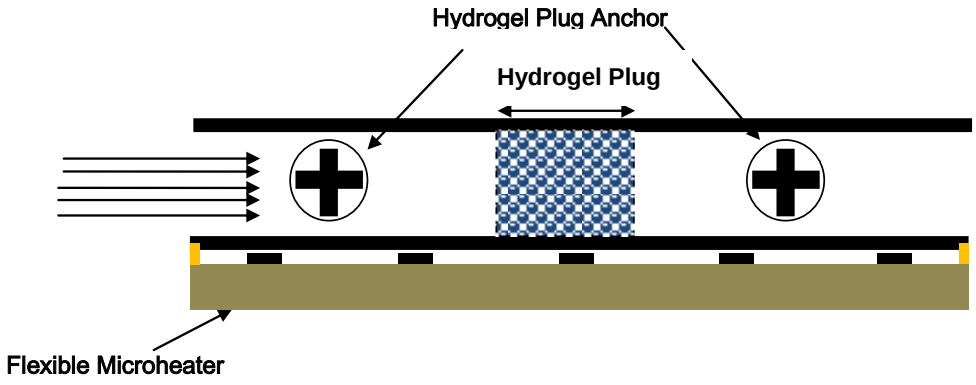

Figure 3-3 The design of the patterened PNIPAAm hydrogel plug of 500 µm square inserted into PDMS channel.

4 .Fabrication of Hydrogel-based microvalve components

4.1 Micromold Fabrication

4.1.1 PMMA Micromold

The laser ablation method is an alternative method to SU-8 photopatterning used to create molds for PDMS molding. This universal system is a CO_2 laser ablation system that uses a laser to cut through various materials. It can be used for rapid prototyping in PMMA or with other materials in microfluidic application. The layout of the heaters was designed using CorelDRAW Version X4. This software is coupled with the UCP (universal control panel), which runs the VersaLaser®. To achieve a depth of 150μm, the system was operated at 100% speed and 80% power intensity. The depth of the mold can be measured using a micrometer. Figure 4-1 illustrates the laser system in Surrey campus. Figure 4-2 illustrates the PMMA micromold with a laser-engraved structure.

Figure 4-1 The laser ablation system in Surrey campus connected to CorelDRAW software

Figure 4-2 Optical Micrograph of Laser Engraved PMMA Micromold

4.1.2 PDMS on SU-8 Molds

SU-8 is the commonly used negative, epoxy-type, near-UV photoresist. It is commonly used in the fabrication of microfluidic structures.
This photoresist can be as thick as 2mm and be patterned in aspect ratios up to 25 with standard UV-lithography.

SU-8 2035 was chosen to make the SU-8 molds. The reason for using SU-8 2035 was because SU-8 2035 can produce relatively high aspect ratio structures as opposed to thinner formulations of SU-8. As our structures were designed to be 110 micrometers in height, this thicker formulation was required. The mask design (designed with LEDIT V13) is shown in Appendix C. The detailed description of the processing steps for making the SU-8 molds is listed in APPENDIX B. One major issue encountered when using SU-8 was poor adhesion. Unfortunately, SU-8 structures on glass came off very easily during de-molding. Cracking also often occurred after the PEB (post exposure bake). It has recommended by researchers that spinning two layers of SU-8 with thickness of 120μm can solve this problem. The thick layer proved to be easy to peel off and handle. Table 4.1 depicts the material properties of PDMS. We can see from this chart that PDMS has high mechanical compliancy, as evidenced by its low Young's Modulus.

Table 4-1 PDMS Material Property

Property	Value
Mass Density	0.97 kg/m^3
Young's Modulus	360-870kPa
Tensile or Fracture	2.24 MPa
Biocompatibility	Nonirritating to skin, no adverse effects on rabbis and mice, only mild in inflammatory reaction when implanted
Hydrophobicity	Highly hydrophobic, contact angle, 90-120°

4.1.2.1 PDMS Bonding

Plasma oxidation (Benchmark 800) can be used to alter the surface chemistry of a material in order to prepare it for bonding. Using this method, PDMS can be easily bonded to other PDMS surfaces, or to silicon or glass. The plasma preparation incorporates the oxygen atoms at the PDMS surfaces. This activation treatment renders the PDMS surface hydrophilic with dangling bonds. RF power, oxygen flow rate, partial pressure, and treatment time were set as independent parameter for the PDMS-PDMS bonding. Adhesion can be a problem with such oxygen bonding if the processing steps are not carefully followed of if the sample is allowed to sit around too long after activation, and can also be caused by non-uniformity of the substrate surface. However, PDMS bonds successfully formed in this manner can be very strong and form liquid-tight seals.

The PDMS was mixed at 10:1 ratio of elastomer/curing agent and then cured at room temperature for 20 hours to increase the viscosity. The PDMS channel to be bonded can also be activated using an Electro-Technic Products Inc. (ETP) BD-20AC laboratory corona treater. This corona treater generates a 10-48 kV, 4-5 MHz electric spark at the tip of its electrode. When the corona treater is powered, it generates a high voltage across the tip of the electrode, ionizing the air, producing a localized corona discharge. The ionized air produces free radicals that react rapidly to form an oxidation layer on the exposed surface of the given PDMS sample thus increasing surface energy and promoting reactive polar groups. The corona treatment can create a dangling hydrogen bonds on the surface. We employ the corona treater to treat the PDMS channel, glass microscope slides.

The corona treater was equipped with 3 electrodes: a straight spring, a one inch disk and 2.5" inch wire. The corona treating can be performed at room temperature without the use of the vacuum system. The corona produced by the spark is adjusted to a relatively low level and subsequently produce a stable and soft corona with minimal cracking and sparking[51]. The spring electrode is utilized then passed back and forth ~1" above the given PDMS sample for ~5 min. A 3 x 1 inch microscope slide can be bonded to pieces of 3x1 PDMS sample within 5 minutes. We also utilized the corona treater to bond PDMS channels with Kapton® microheaters.

4.2 PNIPAAm Hydrogel synthesis and Patterning

Hydrogel synthesis can be made by free radical polymerization of the hydrogel monomer. Free radical polymerization is a method for polymerization by which a polymer forms by the successive addition of the free radical building blocks. In the following sections, we discuss the synthesis and patterning of our PolyNIPAAm gels.

4.2.1 Synthesis of the temperature-sensitive hydrogel PNIPAAm

In order for the thermoresponsive hydrogel to be employed as an actuator, it must be first synthesized. We used N-Isopropylacrylamide(NIPAAM) as the major monomer for our hydrogel synthesis. As reported by other researchers, NIPAM forms a three dimensional hydrogel when crosslinked with N,N'-methylenebisacrylamide(MBAAm)[35].N,N'methylenebisacrylamide(BIS,crosslinker),N'N,N'N'tetramethylethylene-diamine(TEMED,accelerator),acrylamide(AAm, reservoir layer) were all obtained from Sigma Aldrich corporation and employed as purchased. The polyNIPAAm gel was made by free radical polymerization of monomer NIPAAm. The chemical structure of the monomer and crosslinker is illustrated in Figure 4-3. The crosslinking agent MBAAm and monomer NIPAM were first dissolved in de-ionized water (DI H_2O) for 12 hours with a constant supply of N_2 source (oxygen free environment). The initiator APS, and the accelerator, TEMED, were then added to the solution to speed up the polymerization process. All the reagents were contained in 25ml sealed flasks. The polymerization took place immediately after the addition of accelerator TEMED. The polymerization process is relatively fast compared to experiments reported by previous research groups[36]. The weighted percentage of the accelerator TEMED may be the reason for relatively fast polymerization. Gas was formed during the polymerization process. The poly(NIPAM) gel was immersed in DI water for over 12 hours to wash out chemical residues. We then cut the polymerized hydrogel into various sizes to examine its swelling and de-swelling properties(cube shape and cylindrical shape).

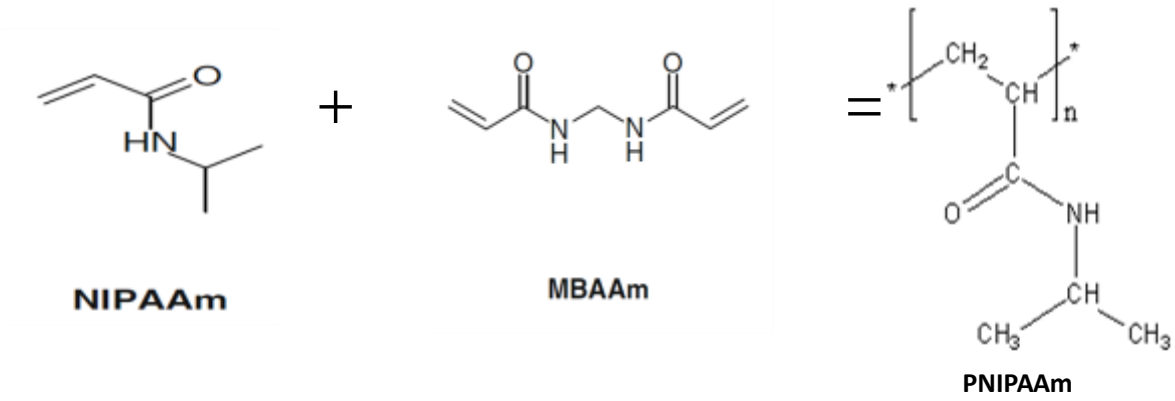

Figure 4-3 Chemical structure of the monomers and cross-linker for the synthesis of the PNIPAAm hydrogel

The detailed weight percentages used for the synthesis of pNIPAAm hydrogel solution described above were:

- Monomer N-Isopropylacrylamide(NIPAAm): 1.5g
- Crosslinker ,N,N'-methylenebisacrylamide(MBAAm): 0.0185g
- Initiator ,ammonium Persulfate:0.08g
- Accelerator: N'N,N'N'tetramethylethylenediamine: 200µl
- Solvent, DI water, 50ml

4.2.1.1 Surface Morphology of the PNIPAAm hydrogel

The surface morphology of the PNIPAAm hydrogel was investigated with a FEI Strata DB235 Field Emission Scanning Electron Microscope (FESEM, FEI Company, Oregon, USA). The FESEM was operated with an acceleration voltage of 5 kV. The hydrogel

samples were freeze-dried at -50 °C first and then were coated with a gold metal layer to improve the surfaces' electrical conduction for SEM imaging. The detailed freeze drying procedure is summarized in Appendix D. Figure 4-4 illustrates the FESEM images of the pore structures in vertical and random orientations based on the different SEM preparation methods (polishing or manual cutting). The average pore size of the hydrogel was 10 μm. These pores were interconnected by thin walls in random directions. The gel volume increased below the transition temperature of 32°C. However, as the temperature increased above the critical solution temperature, the hydrogel was demonstrated to shrink and appear opaque. The swelling of the hydrogel is predominately determined by the internal pore structure. PNIPAAm hydrogel swells relatively slowly compared to other hydrogels (i.e., SPHs, pH-sensitive hydrogel). The porous structure for the hydrogel is important for fast swelling, which is required for closing the valve. The fast swelling of the hydrogel is due to absorption of the water by capillary force rather than by simple diffusion. As illustrated in Figure 4-5, the PNIPAM hydrogel has an average porous structure diameter of 10 μm. The relatively small pores of PNIPAAm hydrogel is the main reason for the slower swelling response time due to the diffusion of water rather by capillary force. SPHs have interconnected pore structures diameters in the order of hundreds of micrometers (resulting in faster swelling time)[37,38].

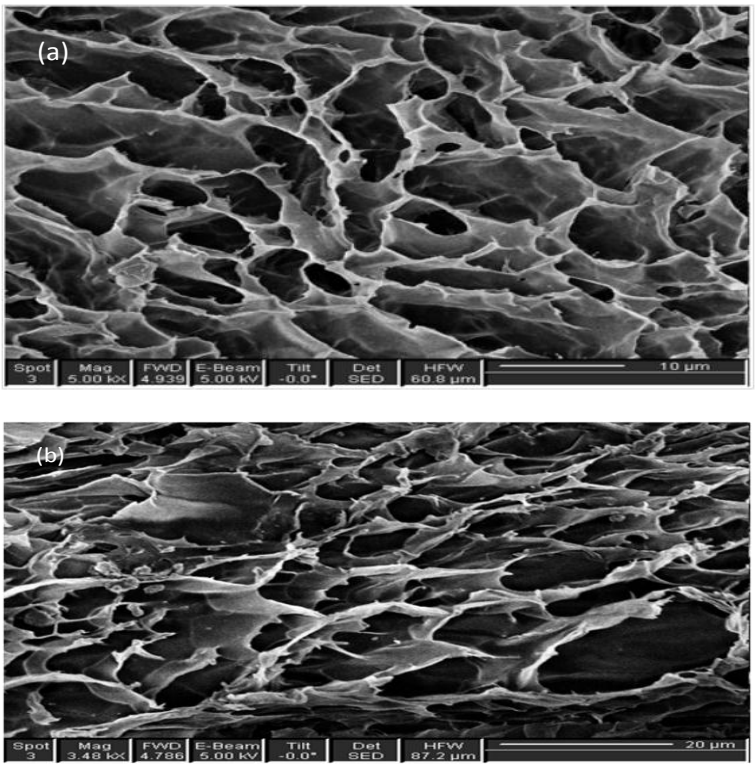

Figure 4-4 Field Emission Scanning Electron Micrograph of the freeze-dried hydrogel membrane with different preparation method : (a) pores are interconnected in the vertical direction with average pore size of 10µm; (b) pores were interconnected in random directions with an average pore size of 20 µm.

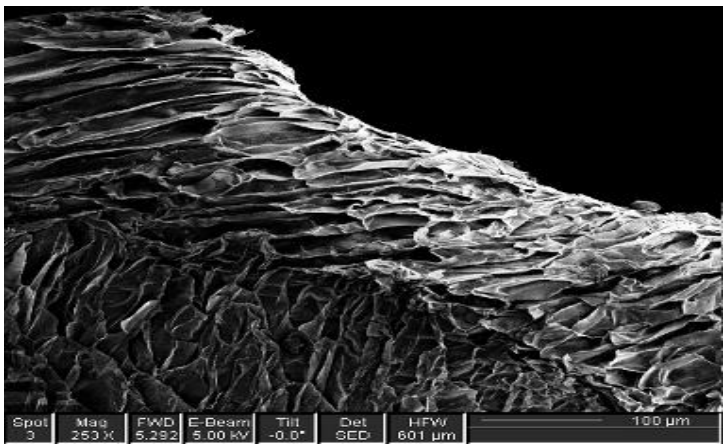

Figure 4-5 Field Emission Microscope Scanning Micrograph of the PNIPAAm at the boundary of the SEM pin stub

Figure 4-5 illustrates the FESEM images of the PNIPAAm hydrogel at the edge of the scanning electron microscope pin stub.

The LCST and phase transition of the PNIPAAm hydrogel depends on the carboxyl group. The amount of element is different for different hydrogel. It is expected that the significant amount of the carbon element is due to the hydrogel's carboxyl group. The amount of carbon element indicates it is PNIPAAm hydrogel. Figure 4-6 illustrates the chemical composition for PNIPAAm hydrogel as characterized by energy-dispersive X-ray spectroscopy(EDX).

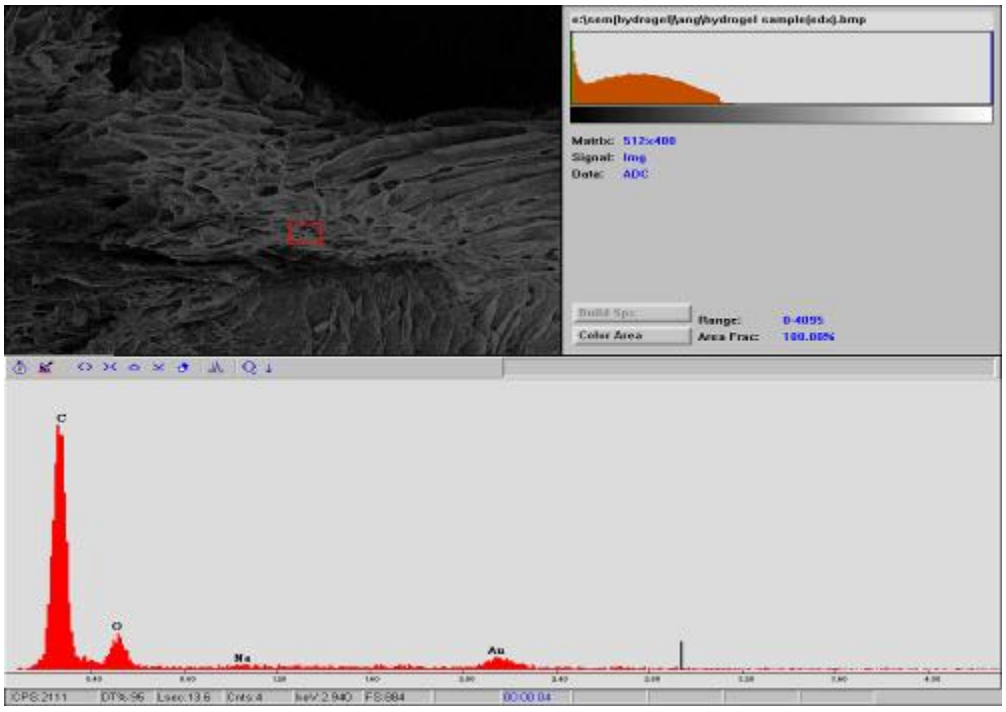

Figure 4-6 Energy-dispersive X-ray spectroscopy(EDX) of the PNIPAAm hydrogel

4.2.1.2 Swelling characteristic of the temperature sensitive hydrogel

Swelling and de-swelling characteristics of the PNIPAAm hydrogel are important parameters for our hydrogel actuator design. Furthermore, degree of swelling can determine surface properties and surface mobility, optical properties, and mechanical properties of the hydrogel. The degree of swelling can take place through two methods: (1) the ratio of sample volume in the swollen state(wet) to volume in the dry state, (2) the ratio of weight of in the swollen state(wet) to the shrunken state(dry sample). Both methods were used to measure the degree of swelling of PNIPAAM over time in our experiment. However, only the first method's results are reported in detail because the second method showed similar results.

The Degree of Swelling(DS) for weight is defined as the mass of absorbed water, as calculated from the weight of the swollen network W_w, per mass of dried copolymer gel W_d :

$$DS = ((Ww - Wd)/Wd) * 100\% \qquad \text{Equation4-1}$$

The mass of the dried gel was determined after the gel was dried on the hot plate at 50 °C for 24h. The dried gel was then immersed in aqueous solution at room temperature until swelling of the hydrogel reached equilibrium. The mass of the wet gel(W_w) was determined after filtering with filter paper. The estimated amount of estimated water filter is depicted in Table 4.1.

The volume of the cylindrical hydrogel plug can be defined by Equation (4-2)

$$V = 2\pi r^2 L \qquad \text{Equation 4-2}$$

We assume that the length of the cylindrical hydrogel plug shrinks the same amount as the diameter; therefore Equation (4-2) can be re-written as the Equation (4-3):

$$V \propto r^2 * \Delta L$$ Equation 4-3

The volume swelling ratio for the gel cylinders can be expressed as the ratio of the gel volume in the equilibrium state(V_1) to the volume at preparation(V_0). This can be measured as the ratio of the respective diameter of the cylinder in the equilibrium state(d) to the diameter at shrunken state(d_0):

$$DS = (V_1 / V_0) = (d / d_0)$$ Equation 4-4

To perform the test, we cut the polymerized hydrogel into cylindrical-shaped (5 mm in diameter, 10 mm long) samples. The hydrogel was placed on a hot plate (50 ºC) in a sealed container filled with water. After about 1 minute, the hydrogel started to shrink and turned from transparent to milky-white. The diameter change of the hydrogel samples was measured under an optical microscope. The de-swelling property was determined by immersing the deformed hydrogel into a cold aqueous solution at room temperature (20ºC). Two independent measurements were made for both the ratio of weight and the ratio of volume method for determining DS. Figure 4-7 illustrates the DS based on ratio of weight. Figure 4-8 illustrates the DS based on ratio of volume of the cylindrical-shaped hydrogel sample. The difference in the two measurements is likely due to measurement error, which includes amount of water not filtered off (in the case of weight measurement) and the error of optical measurement of the distance (in the case of volume measurement).

Figure 4-7 illustrates the weight degree of swelling (the red data points represent the DS with water not filtered completely and blue represents the DS with water completely filtered).

Table 4-2 Weight Degree of swelling

Ww	Wd	Ww-Wd	(Ww-Wd)/Wd	Water(Not filtered)	Ww'	(Ww'-Wd)/Wd
10	1	9	9	0.2	10.2	9.2
9	1	8	8	0.15	9.15	8.15
9	1	8	8	0.05	9.05	8.05
9	1	8	8	0.15	9.15	8.15
8.5	1	7.5	7.5	0.24	8.74	7.74
8.4	1.5	6.9	4.6	0.15	8.55	4.7
8.35	1.75	6.6	3.77	0.2	8.55	3.89
8.3	2	6.3	3.15	0.25	8.55	3.275
8	3	5	1.67	0.15	8.15	1.72
7	4	3	0.75	0.25	7.25	0.8125
5	4.5	0.5	0.11	0.1	5.1	0.13

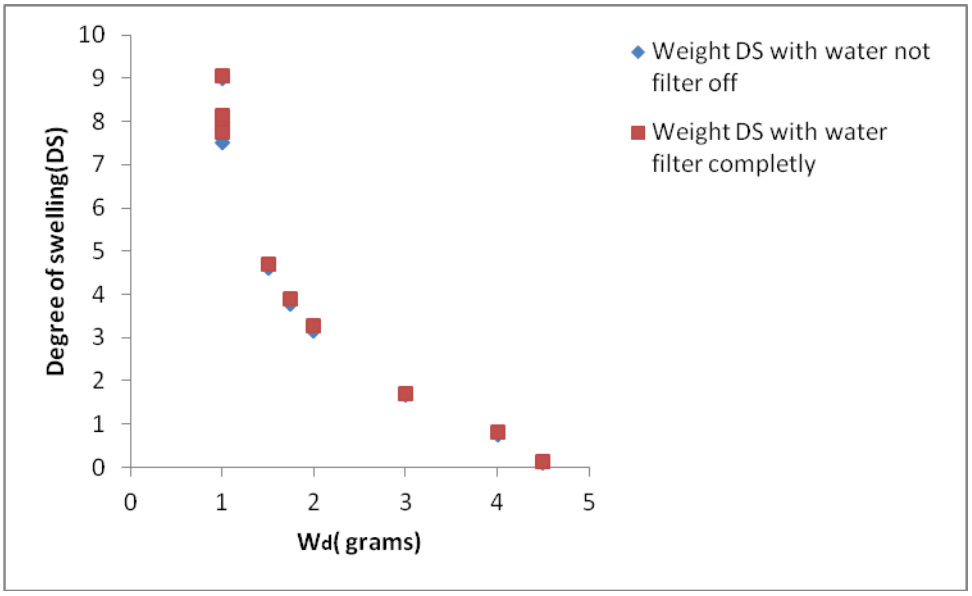

Figure 4-7 weight degree of swelling, The red data points are for DS with sample with water not filter off while the blue data points are for DS with sample with water completely filter off.

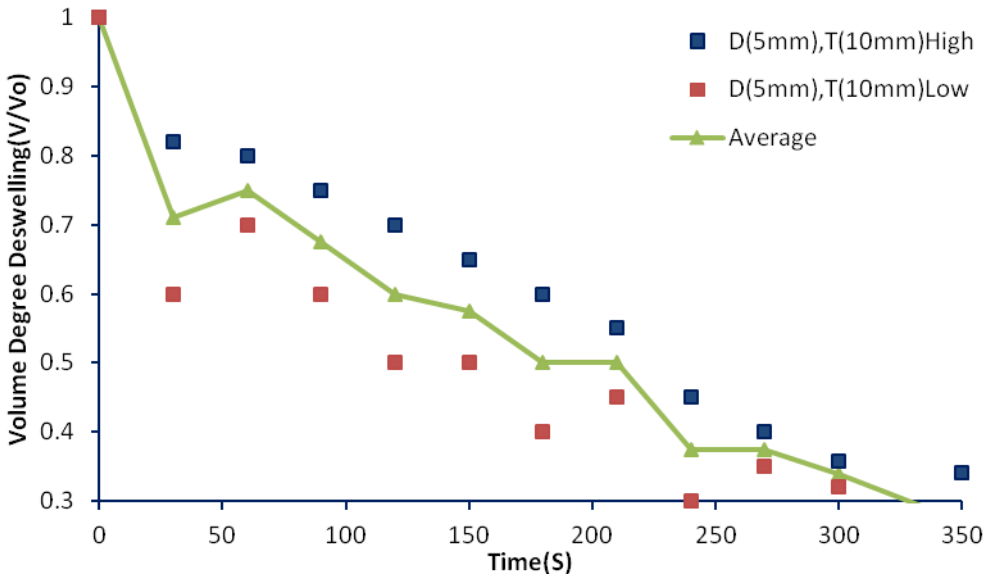

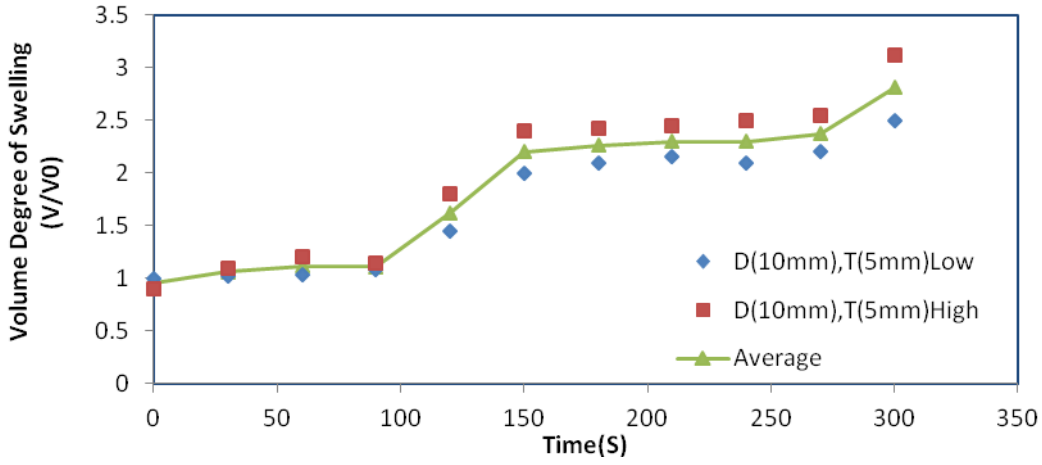

Figure 4-8 (a) Swelling and (b) de-swelling time response characteristics for cylindrical shaped hydrogel sample in response to (a) 50 ºC and (b) 20ºC temperature exposure. The high and low data are representative of two data sets with high and low values of volume DS. The difference between the two sets is due to optical system measurement error.

4.3 Synthesis of pH sensitive, superporous hydrogel(SPHs)

The pH senitive, superporous hydrogel(SPHs) can also be prepared by free radical polymerization of the monomer. All of the chemicals were obtained from Sigma Aldrich Corporation unless otherwise indicated.

Instead of one monomer, SPHs were prepared using a two monomers structure: acrylic acid, acrylamide. The The N'N,N'N'tetramethylethylenediamine(TEMED) and ammonium persulfate(APS) were added at a concentration of 2% to the weight of the monomer, with TEMED being added at the time of polymerization.

Once the monomer solution was made, the pH of the solution was adjusted to 5.0 using sodium hydroxide. This solution was added to a 250 ml flask along with the ammonium persulfate(APS) solution. Sodium bicarbonate was added 210 seconds after adding the APS[40]. Figure 4-9 illustrates the chemical structures of the monomers used for the pH sensitive SPHs hydrogel synthesis.

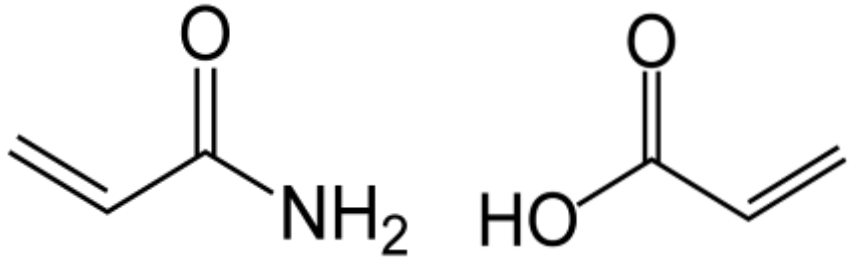

Acrylamide Acrylic Acid

Figure 4-9 Chemical structure of the Monomer(Acrylamide, Acrylic Acid used in synthesis of the pH sensitive superporous hydrogel[41]

The detailed weight percentages used for the synthesis of pH-sensitive superporous hydrogel solution described above:

- Monomer, Acrylic Acid: 1.5g Acrylamide: 10mL aqueous solution

- Cross-linker, N,N'-methylenebisacrylamide(MBAAm):
- Initiator, ammonium Persulfate:0.5 g
- Accelerator, N'N,N'N'tetramethylethylenediamine: 0.5g
- Solvent, DI water, 100 mL

Figure 4-10 illustrates the fabricated pH sensitive and superporous hydrogel. Superporous hydrogels (SPHs) are stronger than the PNIPAAm hydrogel mechanically in terms of material properties(e.g Young's modulus, density) in their shrunken state. The swelling rate is significantly improved, swelling within 20 seconds immersed in aqueous solution as opposed to over 2 minutes for PNIPAAm. The SPHs can be utilized as a normally opened valve due to its large degree of swelling compared to PNIPAAm hydrogel. The SPHs hydrogel can be easily patterned and polymerized *in situ* because the polymerization process can be done without the supply of N_2 source. The normally open valve can be designed to keep the valve seat open by the swollen hydrogel and closed after the shrinking of the gel.

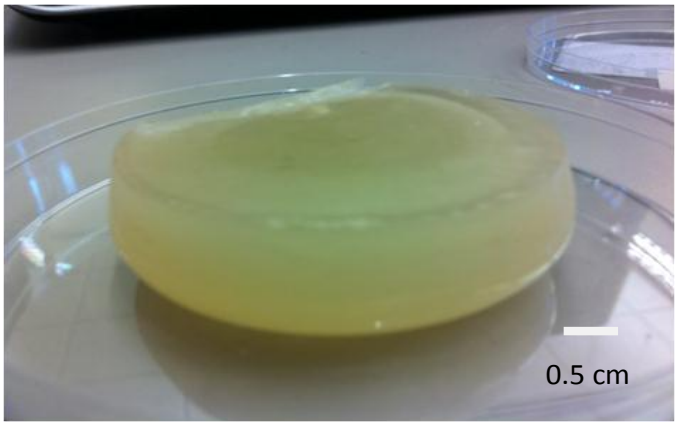

Figure 4-10 Optical Micrograph of the polymerized pH sensitive superporous hydrogel(SPHs)

4.4 PDMS diaphragm Fabrication

A layer of PDMS serves as the actuator diaphragm and as a barrier layer stopping the fluid from penetrating through the reservoir to the microchannel. PDMS has the advantages of high elasticity and easy deformation under actuation. The thickness of the PDMS membrane (suitable range of 100-200μm) is important so that it can be pushed out as the hydrogel swells. We also did not want the diaphragm to be too thin because it proved very difficult to handle PDMS films of a thickness less than 80 μm. To facilitate the desired PDMS membrane deflection of 100 μm, we calculated that a thickness of 80–150μm would be optimal for the PDMS membrane.

To fabricate the PDMS diaphragm, we first manually mixed a 10:1 weight ratio of PDMS prepolymer/curing agent with hexane for one minute, then degassed it for one hour. The PDMS elastomer base was Sylgard 184, which can be diluted up to 40% with hexane to adjust the viscosity and thickness of the resulting PDMS membrane. We silanized the three-inch diameter wafer by applying a droplet of the tridecafluoro-1,1,2,2,-tetrahydrooctyl)-1-trichlorosilane for easy release of the PDMS film. We then dispensed 2–3 ml of the PDMS/hexane mixture with a 14-gauge needle onto the wafer using a 2–20 ml pipette and then spun the wafer using the following set of spin speeds: 500, 1000,1500, or 2000 rpm for 30 seconds. This resulted in a PDMS film of ~100-150 μm on the wafer surface. The wafer was then heated at 85 ºC for two hours on a hot plate to cure the PDMS film. The PDMS film was removed from the wafer by using sharp, curved tweezers. The detailed spin-coating speed versus spin-coating thickness of the PDMS membrane is shown in Figure 4-11. It also illustrates the relationship between the spin speed and resulting spin-coated thickness for the PDMS membrane fabrication.

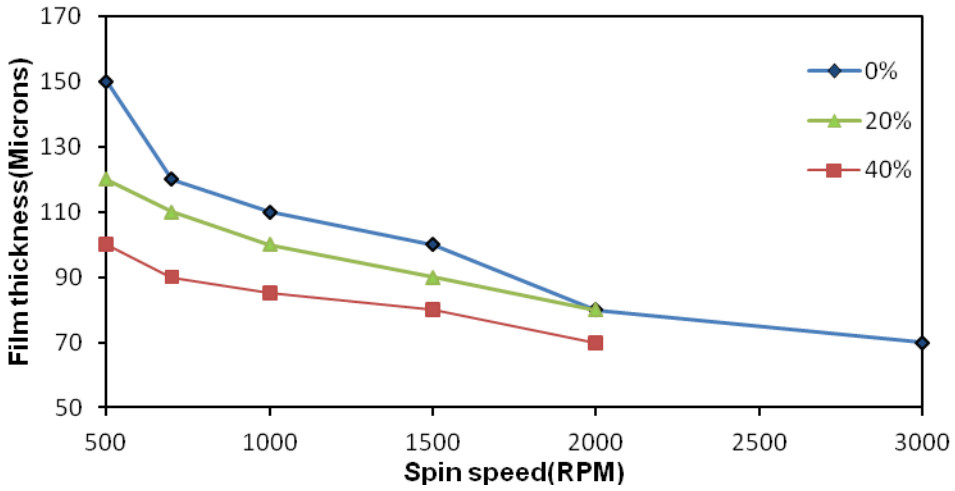

Figure 4-11 Characterization of spin speed and film thickness: 500 rpm,1000rpm, 1500 rpm, 2000 rpm with 0%, 20%, 40% (respectively) hexane dilution of the pre-cured liquid PDMS.

Figure 4-12 illustrates the Scanning Electron Microscope of the ~100 PDMS thick PDMS film used as the deflecting diaphragm into the microchannel.

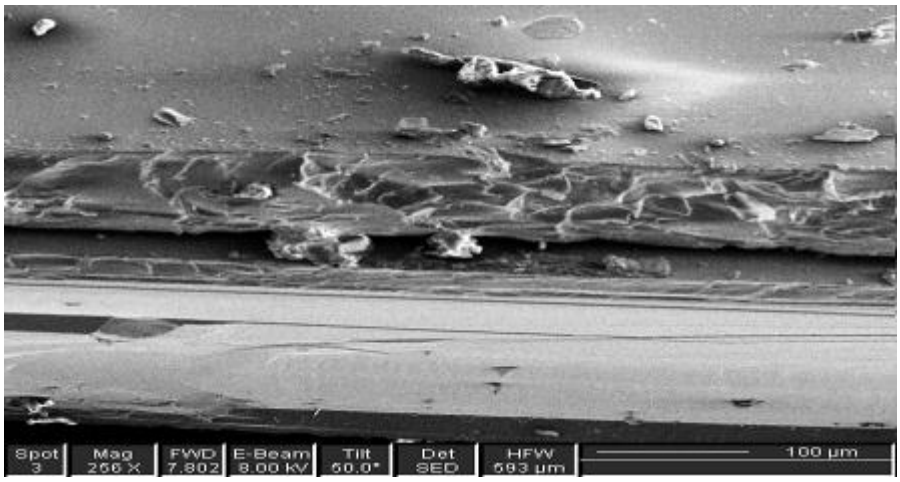

Figure 4-12 Scanning Electron Micrograph of the ~100 µm PDMS Diaphgram

4.5 Hydrogel Micropatterning

Integration of the hydrogels into microdevices requires precise patterning techniques. There are four basic techniques for hydrogel micropatterning:

1. photo-cross-linking
2. micro-molding
3. photo-polymerization
4. particle injection

Initially, the photo-polymerization method was investigated to micro-pattern the hydrogel. Due to the complexity of the hydrogel polymerization *in situ*, we had limited success with photo-polymerization of the hydrogel. Thus, micro-molding was instead used to micro-pattern the hydrogel .

The micromodling technique was utilized to micropattern the hydrogel in the microvalve application. Hydrogel microstructures have been incorporated by other researchers as integral components in microdevices, using photolithography and/or soft-lithography. In order to make hydrogel microstructures in our way, the hydrogel prepolymer was first spin-coated onto a glass/Pyrex™ wafer for 1000 RPM. The thin film hydrogel layer was then compressed between two glass plates and a PMMA mold with the negative of the desired features,; the assembly was then placed into a vacuum chamber for 30 minutes. Figure 4-13 illustrates the detailed schematic diagram for micropatterning hydrogel square structures. Figure 4-14 illustrates the final patterned hydrogel structure of 500 μm wide square and with depth of 1000μm. This significantly improves the precision of the hydrogel insertion into the microchannel and response time compared to the diaphragm microactuator design.

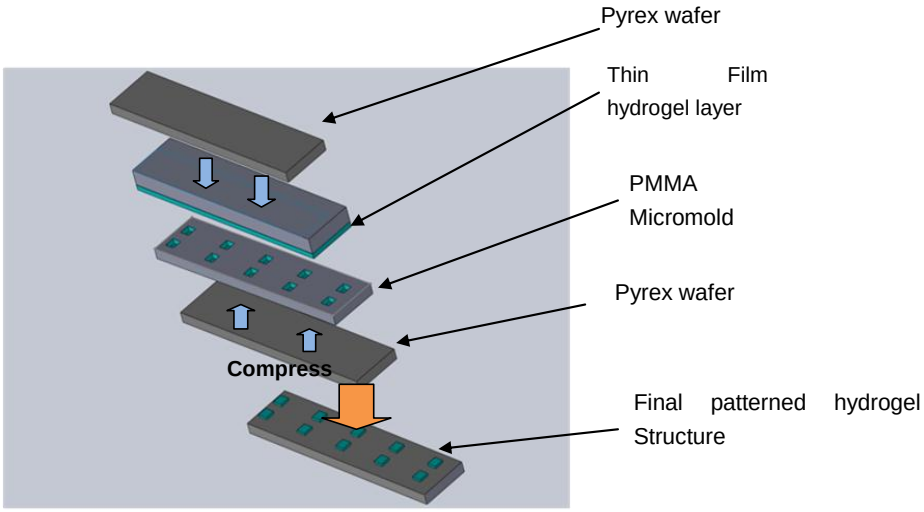

Figure 4-13 Process flow for micro-patterned of Hydrogel

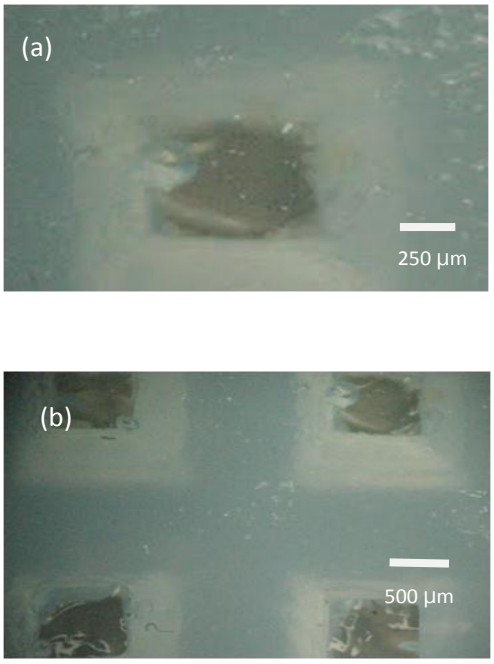

Figure 4-14 Final Patterned Hydrogel Structure

(a) Patterned hydrogel formation on the substrate(500 um) (close up)

(b) patterned hydrogel square array.

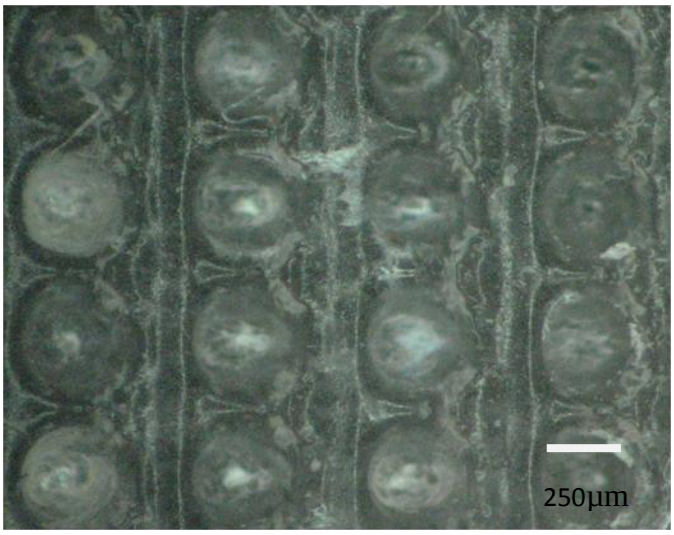

Figure 4-15 Optical Micrograph Micropatterned Hydrogel Cylindrical Structure (250 µm)

Figure 4-15 illustrates the second micropatterning design method using a PDMS micromold with negative feature pattern. The diameters for these cylindrical structures are about 250 µm. Due to the dimension of hydrogel structures, the response time of this cylindrical structure will be faster than the 500 µm square structure , but it will be easily pushed downstream with the fluid(0.2mL/min) due to its size;, therefore an anchor or support structure for this type of cylindrical structure is critical for microvalve realization.

4.6 Microheaters Fabrication

4.6.1 Tungsten C-NCP Heaters

We have made several flexible microheater designs, including those with PDMS as the base polymer and doped with either tungsten (W) or carbon nanotubes (CNTs), and those made by etching foil on Kapton®.

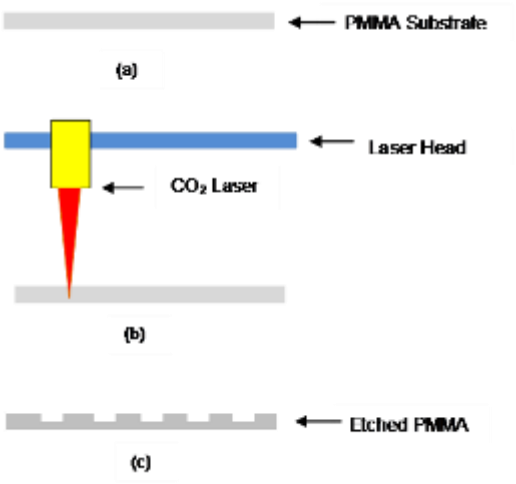

Figure 4-16 PMMA micomold fabricaton steps using VersaLASER© laser ablation system.

Tungsten nanoparticles with an average diameter of 50 nm were purchased from NanoAmor Inc, USA; a PDMS 184 Sylgard kit, which consists of base elastomer and curing agent, was bought from Dow Corning USA. PMMA was obtained from Industrial Plastic and Paint, Surrey, Canada. All the materials were used as purchased.

In order to fabricate the flexible polymer tungsten nanoparticle doped microheaters, micromolds were first fabricated. The micromolds were prepared by laser ablation of cast grade PMMA (Poly Methyl Methacrylate, commercially known as Plexiglass) by using the VersaLASER© laser ablation system which employs a class 3R CO_2 laser diode operating at 650nm wavelength. The layout of the heaters was designed using

Corel Draw version X4. This software was coupled to the UCP (Universal Control Panel) software which runs the VersaLASER© laser ablation system. In order to achieve a depth of 250 μm the system was operated at 100% speed and power intensity of 30%. The depth of the mold was verified using a micrometer. Figure 4-16 shows PMMA micromold fabrication steps. We note that while we used laser ablated molds for the prototype heaters presented in this thesis, was have also been able to fabricate SU-8 micromolds that may be expected to have better feature resolution than the 10 μm resolution associated with the laser ablation process. However, SU-8 molds are not as resilient to the solvents (e.g., heptane) used to assist in uniform nanoparticle dispersion.

After making the micromold, we fabricated the C-NCP heaters using standard soft lithography. Soft lithography is the methods designed to replicate or pattern material like polymers. To make the flexible microheaters, 1.05 grams of tungsten nanoparticles with an average particle size of 30-50nm were first manually stirred in 0.55 grams of PDMS base elastomer for 10 minutes. A horn tip ultrasonic probe was then immersed in the uncured composite operating at a frequency of 42 kHz in pulse mode (10 seconds on and 15 seconds off) for 30 minutes prior to adding curing agent. The base elastomer and curing agent ratio were chosen to be 10:1 respectively as recommended by the supplier (Dow Corning Inc. USA). The prepared composite was placed into a vacuum chamber to remove air bubbles for 30 minutes and poured on to a PMMA micromold and degassed for ten minutes. Excess nanocomposite was scraped off using a Damascene-like process from the surface of the mold using a surgical knife. The step by step fabrication process is shown in Figure 4-17. Undoped PDMS polymer was then poured on the surface and degassed. The substrate was then baked on a hotplate at 60°C for 3 hours and then peeled off from the mold. Figure 4-18 shows an optical micrograph of an example array of fabricated tungsten-PDMS nanocomposite microheaters[42]

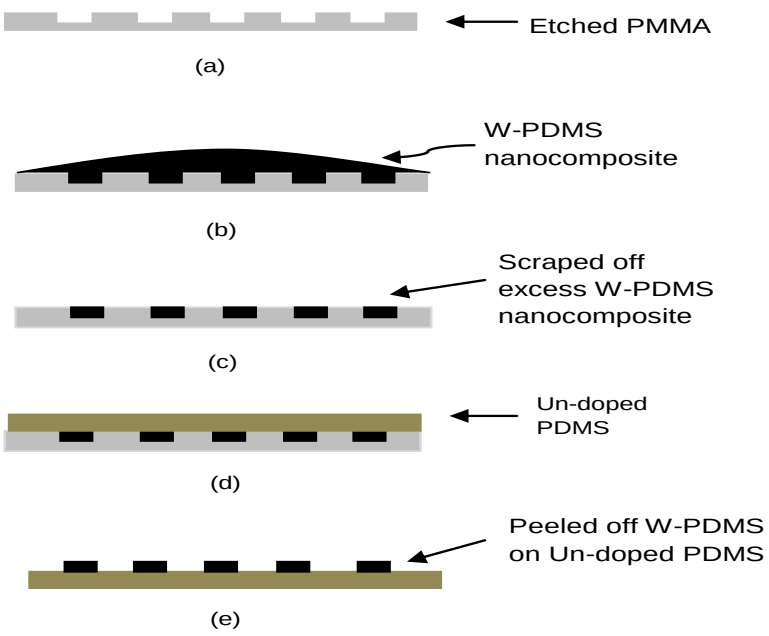

Figure 4-17 Hybrid fabrication process for combining micromolded heaters with nonconductive polymer a) PMMA micromold; b) W-PDMS nanocomposite is poured onto the PMMA micromold; c) excess nanocomposite is scraped off from the surface of micromold; d) PDMS is poured on the surface of mold; e) the resulting W-PDMS microstructures on PDMS nonconductive polymer are peeled from the substrate.

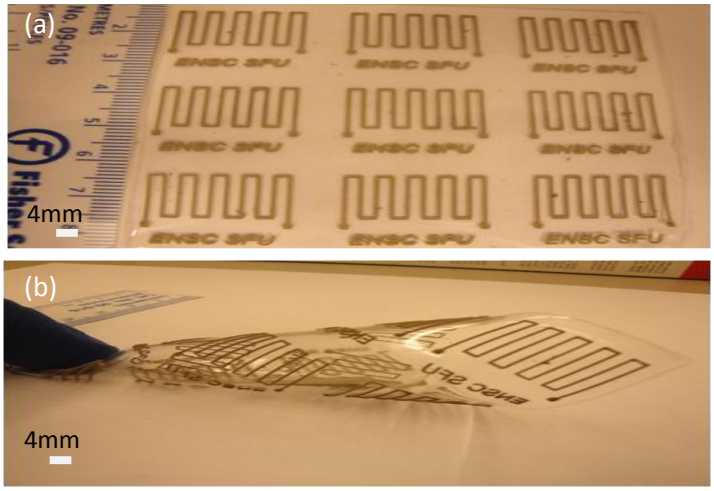

Figure 4-18 Optical micrograph of fabricated W-PDMS microheaters a) heater array element b) showing flexibility (adapted from [39]).

4.6.2 Carbon Nanotubes Heaters

For this thesis, carbon nanotube(CNT) heaters were fabricated by soft lithography. The fabrication procedure is similar to the process described above. Figure 4-19 illustrates the optical micrograph carbon nanotube heaters(CNTs). Uniform heating is one of the major issues for the flexible microvalve application. We found that the carbon nanotube (CNT) heater was not an ideal candidate for uniform heating as heat transmission was to the hydrogel was not sufficient compared to etched foil heater;

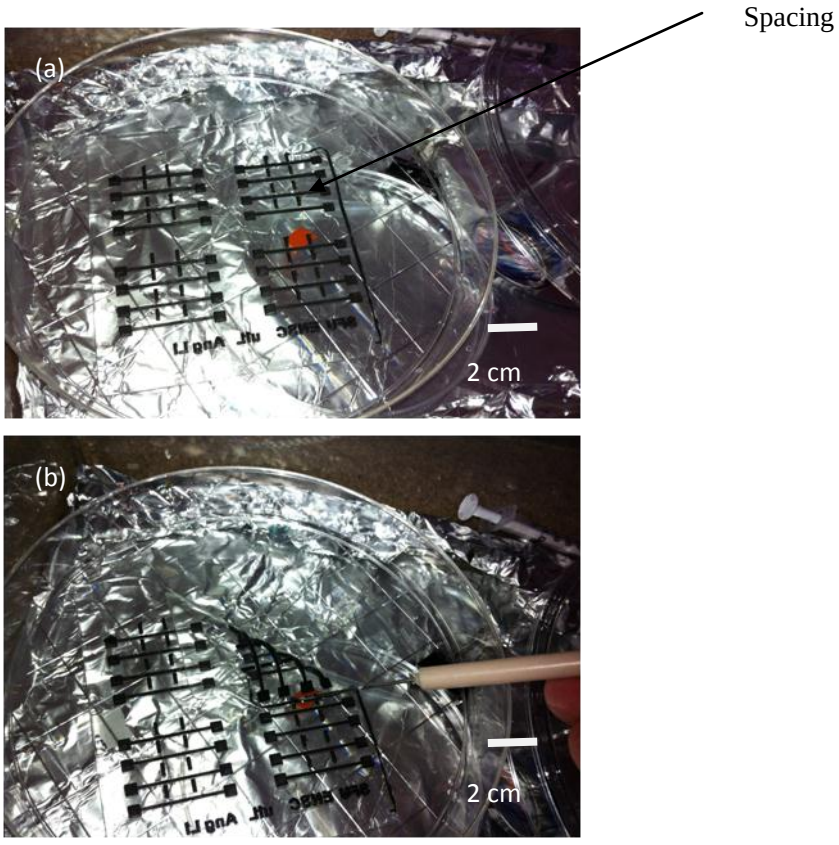

Figure 4-19 Optical micrograph of the fabricated carbon nanotube heater Carbon Nanotube (CNT) heater (a) Fabricated carbon nanotubes heaters (b) showing flexibility

4.6.3 Etched foil heater

Kapton® is a thin, lightweight organic polymer film developed by DuPont that provides excellent tensile strength, tear resistance, and dimensional stability. Kapton® polyimide has excellent physical and electrical properties resulting in thermal stability over a wide temperature range. In order to make the microheaters, the copper foil was etched on the Kapton® polyimide substrate by an industrial grade process based on the specific design parameter (e.g voltage and temperature) for our microvalve application. A photo of the flexible foil heater is shown in Figure 4-20.

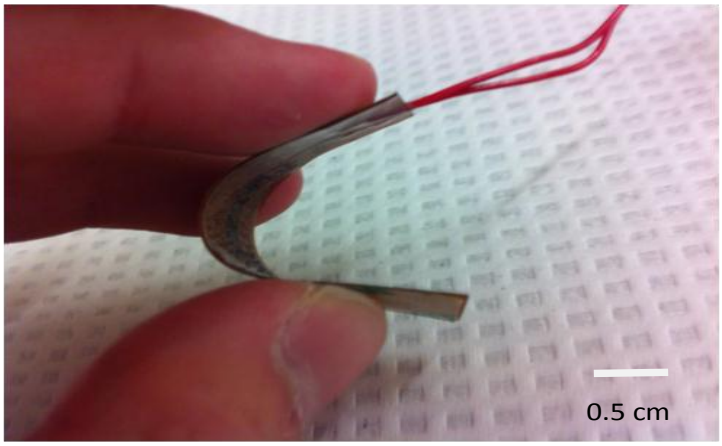

Figure 4-20 Optical Micrograph of the etched foil microheater showing flexibility

5 Testing and Characterization of the Hydrogel-Based microvalve components

5.1 Characterization of the Microheaters

A micromanipulator was used to apply the current to the microheater elements to generate heat. The resistance of the heater element changes linearly with the temperature. The relationship is given by Equation 5-1.

The resistance of the heater element changes linearly with the temperature. The relationship is given in Equation 5-1.

$$R = R_0[1+\alpha(T-T_0)] \qquad \text{Equation 5-1}$$

where R_0 and R are the initial and final resistances; T_0 and T are the initial and final temperatures of the microheater, respectively, and α is the temperature coefficient of resistance. The equation can be rewritten as follows:

$$R = A+BT \qquad \text{Equation 5-2}$$

where $A=R_0(1-\alpha T_0)$ and $B=R_0\alpha$. R can be calculated by evaluating the applied voltage. The TCR (temperature coefficient of the resistance) of the microheater element can be determined by Equation 5.3:

$$\alpha = (1/R)*(\Delta R/\Delta T) \qquad \text{Equation 5-3}$$

where all values can be determined experimentally for deriving of α[50].

The tungsten microheater was heated using a Fisher Thermix Model 210 hotplate. The temperature was measured using a thermocouple connected to an Amprobe 38XR-A digital multimeter, and the resistance was measured using a Fluke 77 digital multimeter. As illustrated in Figure 5-1(a), the resistance of the microheater element increases in direct correlation to the temperature; it thus has a positive slope on the resistance versus temperature graph. The positive temperature coefficient resistance were calculated to be

9.6x10 $^{-3}$/°C, which is comparable to the TCR of pure tungsten (4.5 x10 $^{-3}$ /°C).

To implement the flexible W-NCP PDMS heaters for a thermally responsive hydrogel actuation of a microvalve, we need to determine the exact actuation voltage versus temperature. More specifically, we need to know at what voltage the flexible heaters will produce enough heat to reach phase transition. A micromanipulator (Model # PR0198 Wentworth) was used to apply current to the microheater elements to generate heat. The temperature was measured using a thermocouple connected to a Amprobe 38XR-A digital multimeter. The applied voltage was measured with a Fluke 77 digital multimeter. Figure 5-1(b) depicts the relationship between the temperature and actuation voltage of an example C NCP microheater. As illustrated in Figure 5-1(b) , the C NCP microheater reached the 32–34ºC hydrogel phase transition temperature at a voltage of 13–15 V. We also note that the W-NCP heater exhibits a near linear behavior with respect to voltages up to 25 V and temperatures up to 45ºC.

(a)

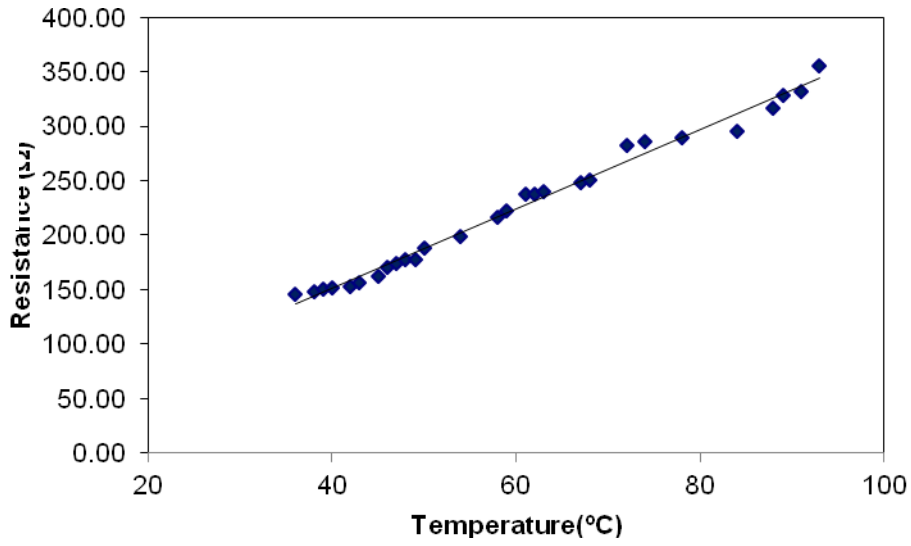

(b)

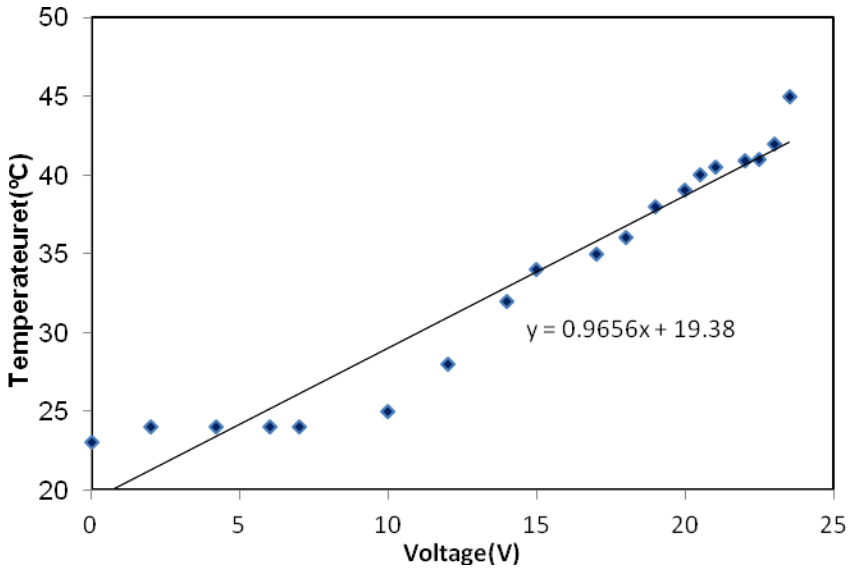

Figure 5-1 Characterization of W C-NCP Microheaters :
a) resistance-voltage correlation for determination of TCR;
b) temperature-voltage correlation

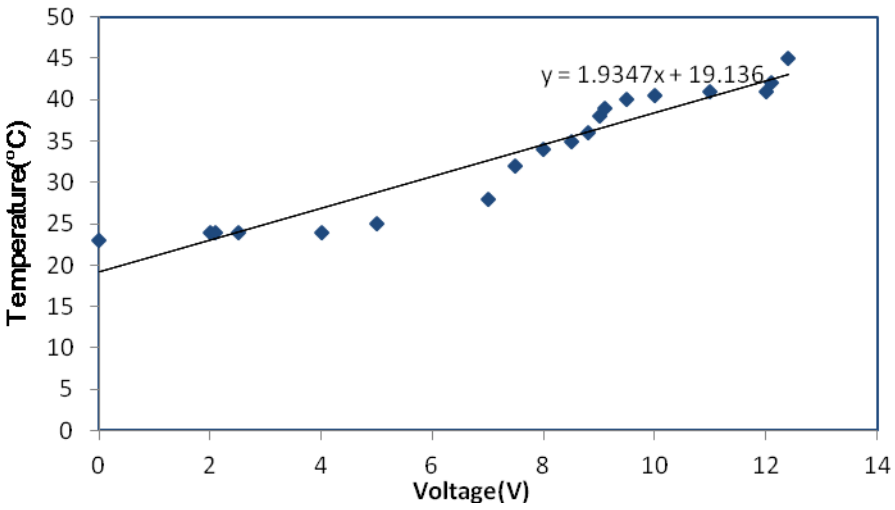

Figure 5-2 Characterization of the CNT Heaters: Temperature Voltage Correlation. We see that the hydrogel phase transition temperature of 32-34 C is reached for an input voltage of 7-9 V.

Figure 5-3 illustrates that the etched foil flexible microheater reached the 32-34 °C hydrogel phase transition temperature with a voltage of 3-5V. Thus, the etched foil flexible microheaters are more efficient than our previous heater designs for hydrogel-based microvalve application, as it reaches the transition temperature at 3V to 5V, rather than more than 10V. The heater is also fabricated using a very inexpensive and commercially available process.

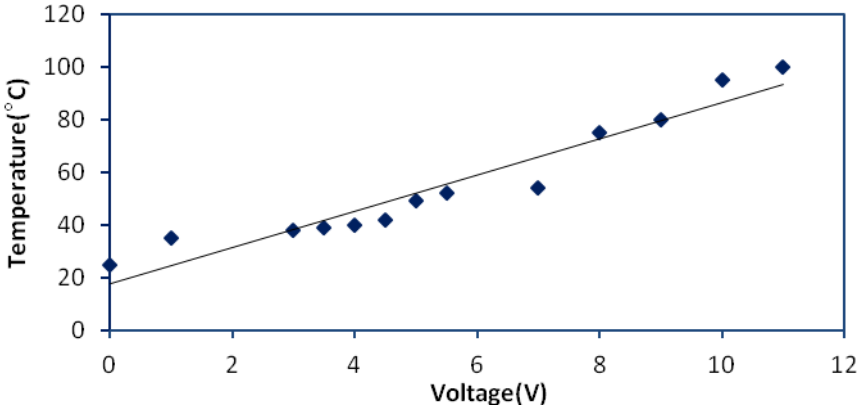

Figure 5-3 Characterization of etched foil flexible microheaters: Temperature-Voltage correlation. We see that 32-34°C (the hydrogel phase transion temperature) is reached for 3-5V.

5.2 Hydrogel-based Microactuator Deflection Result

The thermoresponsive diaphragm-based hydrogel microvalve can be employed for flow control by opening and closing the microchannel by blocking and unblocking the channel with a hydrogel actuated PDMS membrane (microactuator). In this initial study, we present the PDMS membrane deflection results using heat supplied by the novel W-PDMS flexible heaters. The two ends of the C-NCP heaters were connected to a DC power source to control temperature. The PDMS membrane deflection images were captured using a digital camera (Canon Powershot S3-IS) mounted on a microscope (Motic SMZ-168). Figure 5-4 illustrates the state of the PDMS membrane, which was forced to deflect downwards (in the picture) due to de-swelling of the hydrogel in response to heat from the flexible W-PDMS heater. The voltages employed for the heater element were 15-20 V. As seen in Figure 5-3(a) after 30 s of heating, and in Figure 5-4(b) after 1 minute of heating, the color of the hydrogel has turned to a milky white at a temperature of ~40ºC. After removing the power (heat) supplied to the hydrogel, the hydrogel slowly turns from milk white to transparent (taking more than 120 s). In order to speed up the swelling process, a cold aqueous solution (10ºC) was injected with pipette (2-20ml) into the reservoir layer. Figure 5-4(c) illustrates the state of PDMS membrane after cooling/swelling, showing the convex shape due entirely to swelling of the hydrogel. The time for moving the actuator into the "open" valve position (de-swelling) was relatively faster than moving it into the "closed" valve position (swelling). Based on the times required for membrane deflection, the average time for opening a microvalve employing this membrane actuator (via de-swelling) would be 30 seconds and the average time for "closing" the valve (swelling) would be 120 seconds.

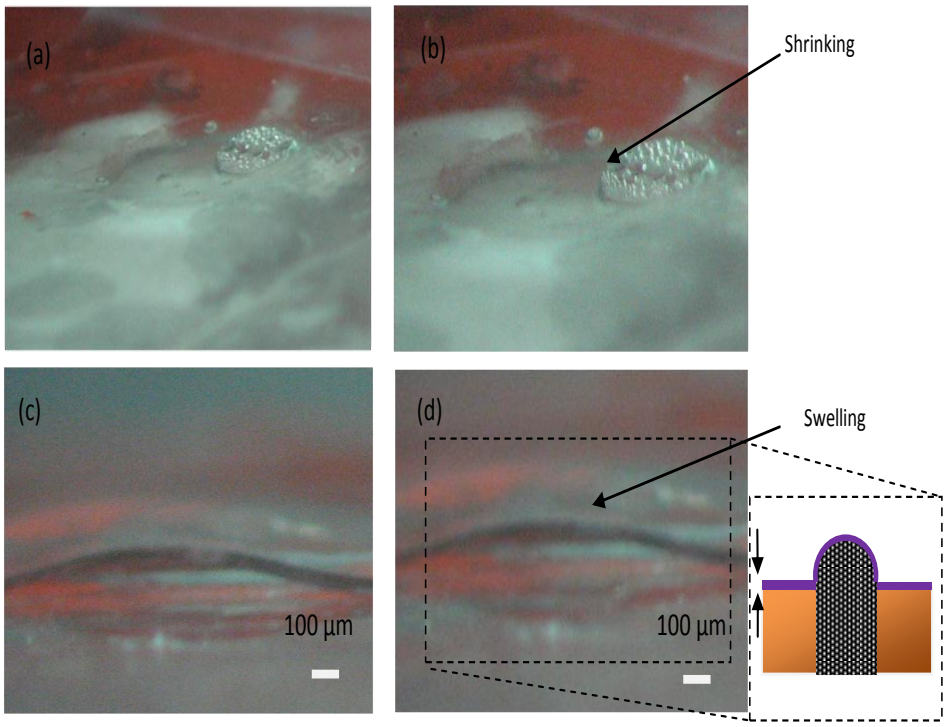

Figure 5-4 PDMS membrane actuated by employing flexible W-PDMS C-NCP heater for hydrogel thermal response (membrane thickness ~100 µm)(a) (a) Hydrogel starts to shrink immediately on the flexible microheater, causing the fluid temperature to exceed the volume phase transition temperature of 32ºC; the valve was opened after 30 seconds of heating, (b) the state of PDMS membrane after one minute of heating at 40ºC, (c) hydrogel was swollen by injecting a cold aqueous solution (10ºC) into the reservoir, and d) the state of PDMS membrane after four minutes of initial cooling at room temperature. Figures (c) and (d) show an estimated deflection of ~100 µm.

5.3 Plug-type Hydrogel-Based Microvalve Fluidic Control Result

5.3.1 Basic Microchannel Fluidic Theory

In order to understand the fluidic behavior and model fluidic flow in the microchannel, fluidic mechanics theory needed to be discussed first.

Reynolds number is important parameters for fluidic mechanics. Reynolds number is used to determine if a flow is laminar or turbulent. Reynolds number can be defined by Equation.(5.4).

$$R_e = \frac{\rho v L}{\eta} \qquad \text{Equation 5-4}$$

where L is the hydraulic diameter of the microchannel, v is the velocity of the fluid(m/s), ρ is the density of the fluid(kg/m^3), and η is the dynamic fluid viscosity(kg/ms). If the Reynolds number is smaller than 2000, the fluid flow is generally considered laminar. If the Reynolds number is greater than 2000, it is generally considered to turbulent.

Entrance length is the distance between the channel from the entrance to where fluid reaches laminar flow. The entrance length can be defined by the Equation (5.5).

$$\frac{L_e}{d} \approx 0.06 R_e \qquad \text{Equation 5-5}$$

where L_e is the entrance length(m), d is the channel diameter, R_e is the Reynolds number.

The head loss(Δh_L)is due to friction in the channel. The head loss in the microchannel can be defined by Equation (5.6).

$$\Delta h_L = f \frac{L}{D} \frac{v^2}{2g} \qquad \text{Equation 5-6}$$

where L is the length of the channel, D is the hydraulic diameter, g is the gravitational constant and v is the fluidic velocity.

Pressure drop describes the pressure loss due to friction in a channel or pipe. High velocity results in a high pressure drop. The pressure drop in the microchannel can be defined by Hagen-Poiseuille equation(Equation 5.7)

$$\Delta P = \frac{128\mu L}{\pi D^4} Q \qquad \text{Equation 5-7}$$

The fluidic resistance in the microchannel can be defined by Equation.(5.8)[52].

$$R = \frac{128\mu L}{\pi D^4} = \frac{8\mu L}{\pi R^4} \qquad \text{Equation 5-8}$$

Figure 5-5 illustrates the basic fluidic testing setup for characterization of these hydrogel-based microchannel microvalves. The second valve design was tested for its ability to function as a valve with constant flow rate of liquid(0.3mL/min) supplied via the syringe pump.

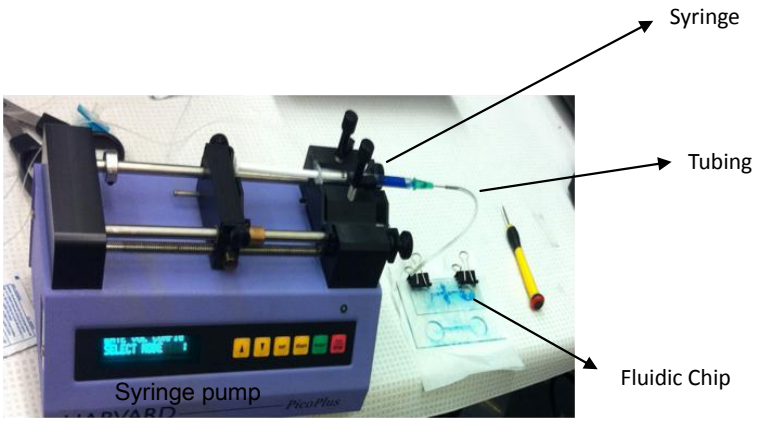

Figure 5-5 Experimental Setup for testing hydrogel-based fluidic control in a microchannel

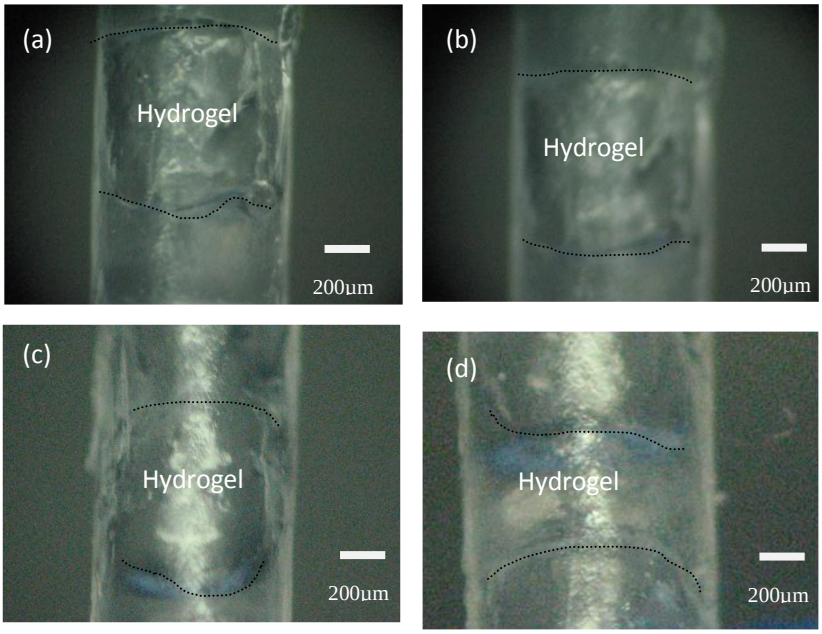

Figure 5-6 . The hydrogel plug confined in polyethylene tube of 0.58mm diameter

(a) thermo-sensitive hydrogel plug at room temperature;
(b) thermo-sensitive hydrogel plug at 28°C for 10 seconds;
(c) thermo-sensitive hydrogel plug at 32°C for 15 seconds;
(d) thermo-sensitive hydrogel plug at above 32°C for 30 seconds.

The first gel design was characterized by flowing liquid through the tubing using a source syringe pump (Harvard Apparatus '11') with a constant flow rate. Figure 5-6 illustrates the state of the hydrogel plug with constant flow rate of 1 mL /min and no applied heat (microvalve "closed"). In order to open the microvalve, the polyethylene tube with hydrogel plug, was fixed to the flexible microheater, which was set to a temperature above 32ºC. As illustrated in Figure 5-6(d), the microvalve plug lifted up approximately 200 µm which partially opened the valve allowing the fluid pass through. To close the valve, the polyethylene tubing was allowed to cool to room temperature (24° C) in approximately two minutes.

Figure 5-7 illustrates the flexible hydrogel-based microvalve setup for a hydrogel plug placed inside a micromolded microchannel rather than a commercially available tube. The PDMS microchannels were bonded on top the flexible microheater as illustrated in Figure 5-7. The polyethylene tubing was glued to the PDMS microchannel.

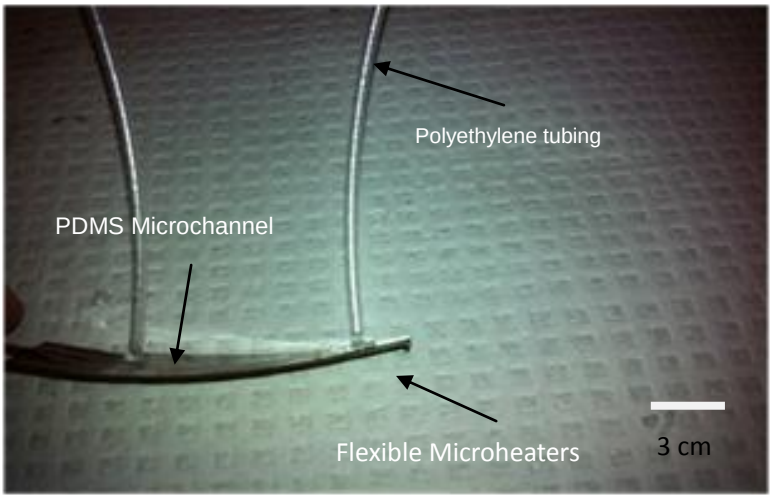

Figure 5-7 Flexible Microvalve Setup

Figure 5-8 shows the results of this testing based on the setup of Figure 5-7. As seen in Figure 5-8 (a), the hydrogel valve initially completely blocks the flow of the blue fluid in the channel as no heat or power is supplied to the hydrogel; however, upon application of heat, the hydrogel immediately starts to shrink. After 10s of heating above the hydrogel phase-transition temperature of 32°C with an actuation voltage of 5V, Figure 5-8(b) results. The hydrogel plug quickly shrinks by approximately 200 μm, allowing the fluid to pass through. The hydrogel plug of 500 μm completely opened the channel within 20 seconds (Figure 5-8(d)). This result is comparable to 30 seconds required for a PDMS diaphragm to deflect 100 μm due to hydrogel shrinkage in our previous design[42]. Thus, this new valve allows for greater opening in a shorter amount of time compared to the previous design.

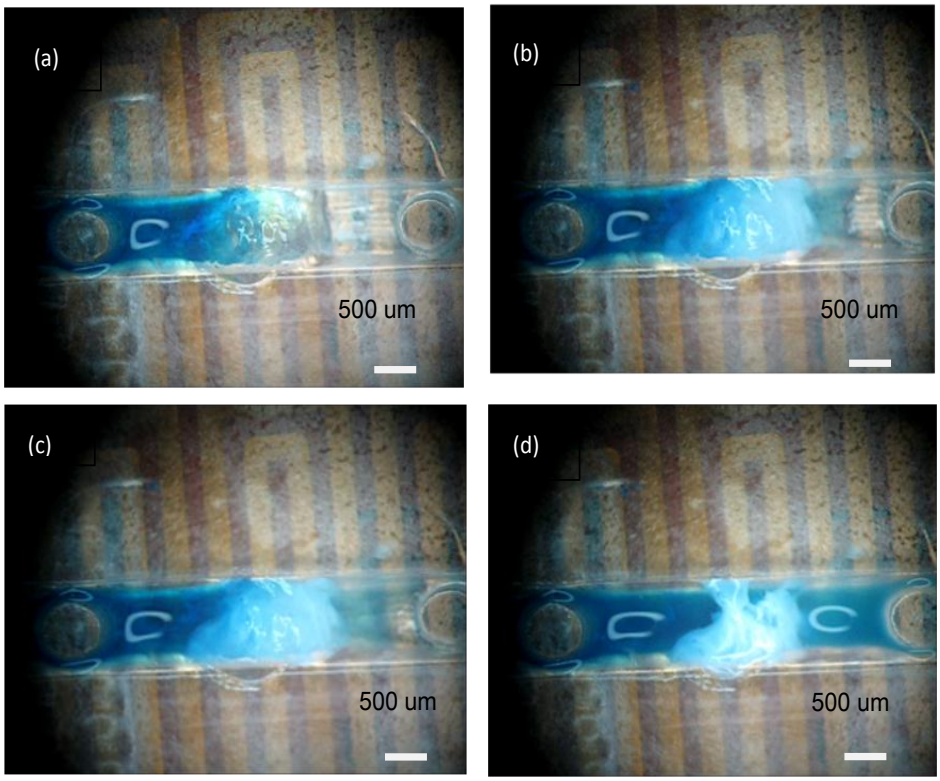

Figure 5-8. Thermally actuated hydrogel-plug in PDMS microchannel(normally closed thermally responsive microvalve design blocking blue liquid from the left): (a) hydrogel starts to shrink immediately upon the application of power to the flexible microheater heating, resulting from the hydrogel structure exceeding the volume phase transition temperature of 32 °C; this photo was taken just as the heat was applied; b) The microvalve after 10s; (c) microvalve after 15s of heating; (d) micro valve after 20s, with valve open and allowing fluid to pass.

5.4 Characterization of the hydrogel-based microvalve

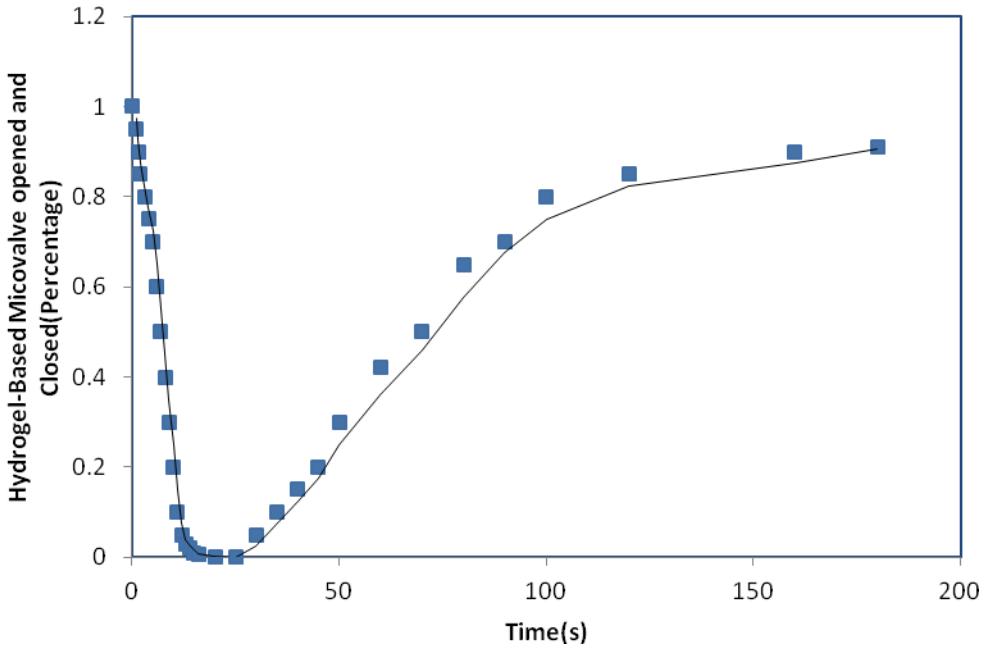

Figure 5-9 Time response of the valve(opening and closing)

Figure 5-9 illustrates the time rate of response of the gel plug opening and closing. The gel shrinks and opens the valve within 20 seconds and expels its most of its water mass. The hydrogel PNIPAAm becomes hydrophilic and regains its shape via diffusion for more than two minutes. Our hydrogel-based microvalve are very repeatable, it can be tested using 4-5 cycles of opening/closing.

The breakdown pressure of the hydrogel-based microvalve was measured by flowing fluid with different flow rates (0.3mL/min to 1mL/min, in the absence of heat). The constant flow rate of 1ml/min was be used until the gel plug's pressurization limit was reached. This result was further confirmed by the gel plug simulation in chapter 6. The gel plug pressurization limit can be defined as the pressure that causes the gel plug to deform. The gel plug failed when the flow rate was equal to 1.0mL/min in our experiment after 10 seconds. As illustrated in Figure 5-10, the maximum pressure that gel can hold is 2010 Pa. Beyond this point, it starts to deform, and the gel plug will be flushed downstream.

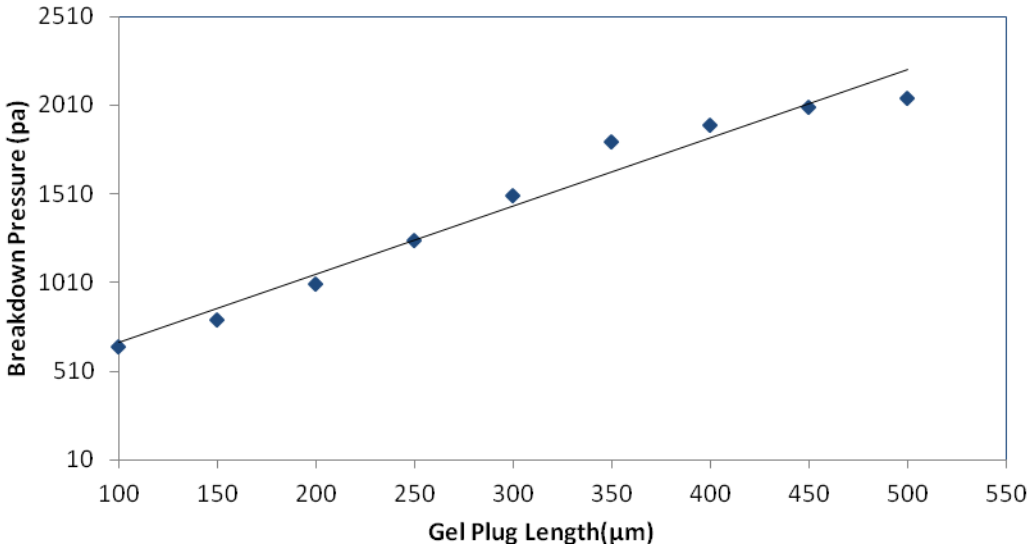

Figure 5-10. The pressure tolerance of the gel plug as a function of the gel's length

6 Simulation

6.1 Hydrogel-Based Microactuator Simulation

The setup of Figure 3-1 and results depicted in Figure 5-1 can be modeled and simulated by COMSOL® Multiphysics which included the thin PDMS diaphragm. A PDMS diaphragm, between 200-400 μm in diameter, was deflected to 100-200 μm via thermally controlled contraction and expansion of the hydrogel, with heat was provided by a mechanically flexible polymer heater, with the entire valve structure also being flexible. On-going investigations by various researchers are examining the possibilities of coupling of the two modules (the structural mechanics module and the microfluidics module) and solving them simultaneously for PDMS diaphragm deflection simulation. This simulation for membrane-based microactuator can support the validity of the fabricated model.

6.2 Hydrogel Plug Design Simulation

The hydrogel plug microvalve designs were simulated using the fluidic structure interaction module (FSI); this multiphysics interface is used to model the interaction between the fluidic and solid structures. The fluidic flow in the channel is described by the imcompressible Navier-Stokes equations(Equation 6.1) for the velocity field.

$$\rho(\frac{\partial v}{\partial t}) - \nabla\{-P\mathrm{I} + \eta[\nabla v + (\Delta v)^t + \rho v * \Delta v = F \qquad \text{Equation 6-1}$$

where density ρ =1000 kg/m^{-3} , P is the pressure of the fluid, η is the dynamic

viscosity, F is the volumetric body force acting on the fluid, v is the fluid velocity, and I is the identity matrix. In most microfluidic simulations, erroneous results are obtained as they exclude the boundaries that have an effect on flow; the additional term F= -12 ρ v d^{-2} is added to Equation(6.1) to rectify this error. COMSOL® solved Equation(6.1) using the Generalized Minimal Residual Method(GMERS) solver.

Equation (6.1) was constrained by the following boundary conditions: (1) no-slip boundary condition, v =0; (2) normal pressure must be perpendicular to the boundary; (3) non-zero pressure inlet; and (4) zero outlet pressure.

The COMSOL® software provides two methods for performing FSI: one-way coupling and two-way coupling. The two-way coupling method was utilized for COMSOL Arbitrary Lagrangian- Eulerian (ALE). Thus, the fluid and solid physics were solved concurrently.

The PNIPAAm hydrogel material properties were modified accordingly for this simulation. The heater elements were not incorporated within the simulation model, although we hope to incorporate this into future simulations. The plug materials of the simulated microchannel was set with the hydrogel material properties (e.g., Young's modulus, Density, Poisson's ratio). This model simply demonstrates the shrinking and swelling capability for the microvalve application.

The theoretical value of mean velocity within the channel of 500 μm square cross section were computed. First, the fluidic resistance of our simulated channel were obtained using Equation (6.2)[43].

$$R = \frac{128\mu L}{\pi D^4} = \frac{8\mu L}{\pi R^4} \qquad \text{Equation 6-2}$$

where D is the hydraulic diameter of the channel, μ is the fluidic viscosity, and L is channel length. Hydraulic diameter(D) was calculated to be $\approx$0.561 mm for the 500μm cross-section channel and the $R \approx 4.04\text{x}10^8$ (s^2/m^5). The theoretical value of the mean

velocity was obtained by solving Equation(6.3). Equation (6.3) describes the relationship between pressure drop and fluid velocity:

$$V_{theo} = \nabla P / AR \qquad \text{Equation 6-3}$$

We calculated the theoretical value of the mean velocity in the simulated microchannel to be 0.19m/s. Figure 6-1 illustrates the hydrogel plug design simulation in a square cross section of the microfluidic channel. Figure 6-1(a) illustrates the hydrogel-based microvalve in a closed position as the hydrogel plug swelled. Figure 6-1(b) illustrates the microvalve in an open position as the hydrogel plug shrinks due to thermal energy. The pressure drop in the simulated channel is 20Pa. The mean velocity in the open channel position (hydrogel shrinking) solved by COMSOL® is 0.17 m/s as illustrated in figure 6-1(b), which is comparable to our calculated value of 0.19m/s, and in the range of our experimentally applied values. We further characterize the pressure breakdown of the hydrogel plug. As illustrated in Figure 6-2(b), the hydrogel plug started to deform or pushed downstream as the inlet velocity reached 0.0667 m/second (volumetric flow rate of 1mL/minute), which confirms our finding on the gel plug pressurization test in chapter 5.6. The experimental pressure tolerance will be compared to the simulated pressure tolerance in future simulations. This comparison will help us gain a better understanding of the pressurization limit of such hydrogel-based microvalve towards developing a fully working device. Additionally, the heater element will also be incorporated

(a)

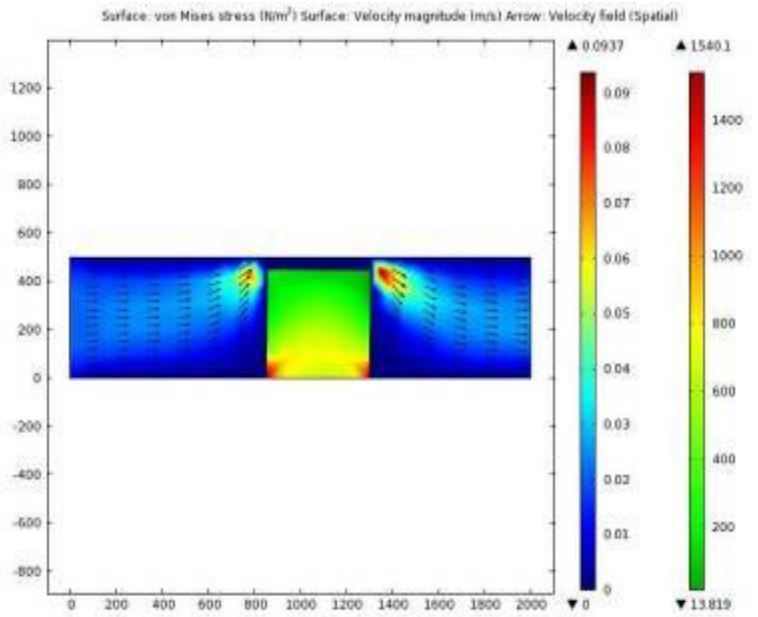

(b)

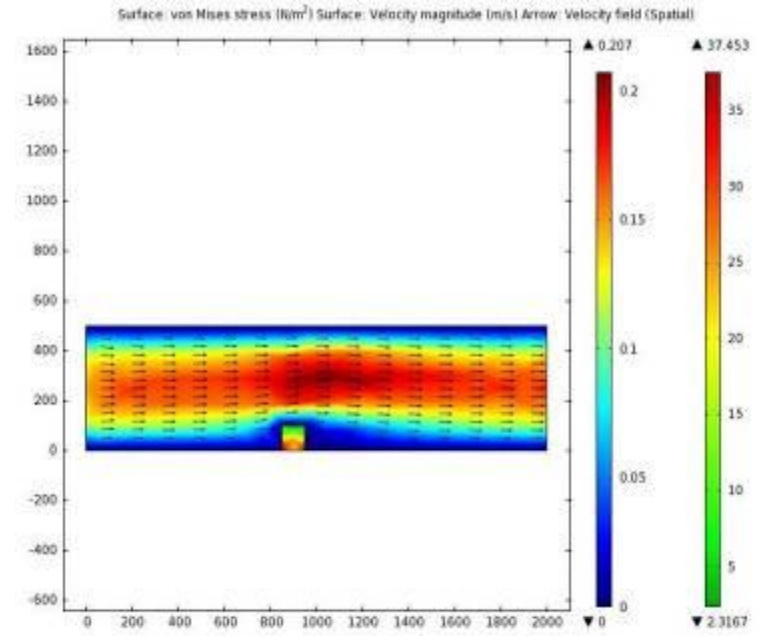

Figure 6-1 Simulation of the hydrogel plug design as a fluidic control element within a microfluidic channel of 500 m (a) as hydrogel plug swells, it blocks the channel; (b) shrinking of hydrogel plug allowed the fluid to pass through with mean velocity of 0.17 m/s.

(a)

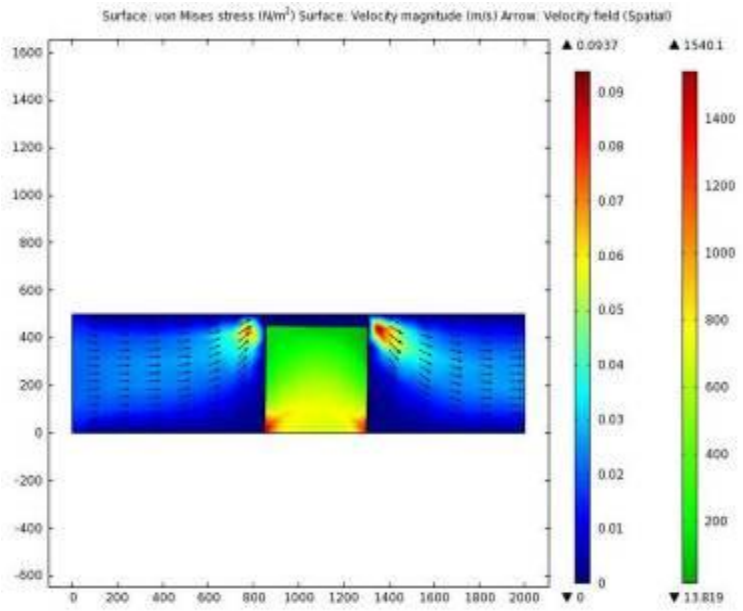

(b)

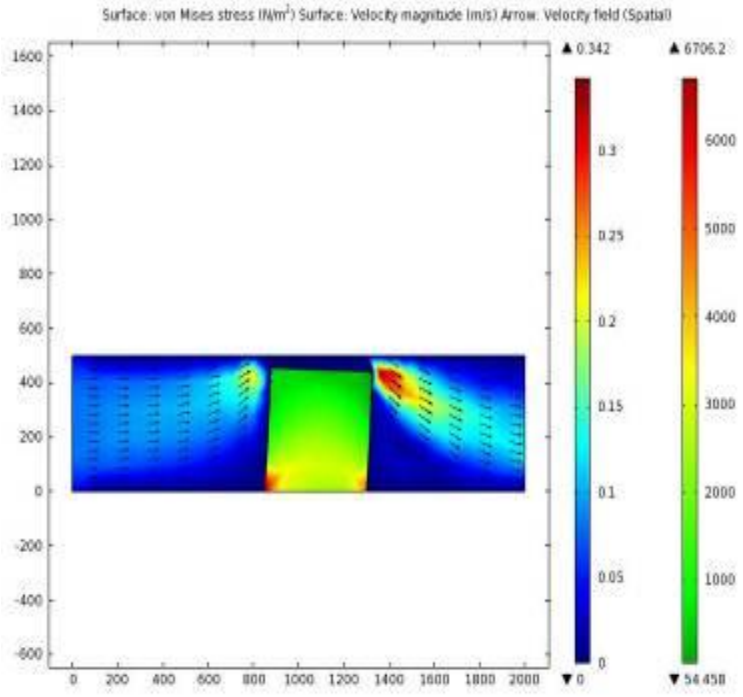

Figure 6-2 Simulation of the hydrogel plug design within a microfluidic channel of 500 µm: (a) the inlet flow rate 0.3mL/min; (b) the inlet flow rate 1mL/min caused the hydrogel plug to fail or deform.

7 Potential Application

7.1 Drug Delivery

The PNIPAAM hydrogels are temperature-responsive polymers. There are large numbers of temperature-responsive drugs that can be delivered in these dosage forms. There is a approach to develop a reservoir type microcapsule drug delivery system by encapsulating the drug core with ethylcellulose containing nano-sized PNIPAAm hydrogel particles[45]. Thermosensitive monolithic hydrogels were used to obtain on-off drug release profile in response to a stepwise temperature change. Temperature-sensitive hydrogels can be secured by placing them inside a rigid matrix by grafting them to the surface of rigid membranes[45]. Our flexible valve utilized PNIPAAm hydrogel can test up to 1ml/min which is useful for most drug delivery[47].

X.Cao et al[46] utilized a pH sensitive hydrogel poly(MAA-co-EG) to perform drug delivery. The hydrogel can expand or contract as the surrounding pH changes, thus cause the release channel to open and diffuse drug in a controlled manner. Even though this work is based on non-flexible substrates which is different from the designs presented in this thesis, it serves as an example application platform for developing future flexible drug delivery device.

The other potential drug delivery platform was based on a microneedle array[50]. The integration of the hydrogel microstructure into the microneedle is probable because the hydrogel is highly biocompatible. The aim is to produce a hydrogel-based microneedle actuation that could be employed to self-administered drugs without supervision of medical personnel.

8 . Conclusion and Future work

Two designs for a mechanically flexible, hydrogel-actuated valve have been introduced which employ flexible polymer heaters (C-NCP or etched foil). The first microactuator design utilized a thin PDMS diagram which deflects from hydrogel swelling with fluid from a separate reservoir. The flexible, doped polymer, microheater elements were characterized. In addition, the voltages required for phase transition temperature of the hydrogel were determined for NCP microheaters. Preliminary experimental results showed that the PDMS membrane actuated by thermo-responsive behavior of stimuli-sensitive hydrogel has an average of 100 μm deflection. Although the microvalve actuator results were preliminary, results indicate that the combination of PNIPAAm hydrogel and flexible, nanocomposite, polymer heater element is suitable for flexible microvalve fabrication. The predicted valve-opening time (de-swelling) is expected to be faster than closing time (swelling), although both times are slow compared to those of many microvalves (although on-par with a number of microvalves based on hydrogel thermal response[43]).

This thesis also presented progress in the development of in-plane hydrogel-based microvalves for flexible microfluidic platforms. The second microvalve actuator design utilized a smaller in-plane gel plug as a fluidic control element in the microchannel. Fabrication of the hydrogel-plug actuators, including the micromolding of the hydrogel thin film, was presented. Microfluidic simulation of the plug in channel design, and experimental testing, including demonstration of valve action and pressurization limits, supports the validity of the microvalve designs. The hydrogel response time was improved over that of the diaphragm valve by micropatterning the bulk hydrogel and precisely inserting it into the microchannel, resulting in a 20 second response (as opposed to 30 second) for similar deflection amount. The results indicate that the hydrogel in-plane plug design is suitable for flexible microvalve applications; it shows

improvement over the micro-actuator design.

The repeatability of the proposed hydrogel-based microvalve should be further researched. One solution for repeatability is that the shrinking PNIPAAm gel can swell back to original shape via diffusion, but this requires photo-polymerization *in-situ* which can result in smaller patterned structure 100 μm. Another solution is that the integration of micro-patterned superporous hydrogel(SPHs) into the microchannel can result in faster closing time of the valve as opposed to PNIPAAm hydrogel.

Also, as meantioned previously, for the in-plane microvalves, as the fluid in the microchannel in incorporated into hydrogel swelling, the fluid parameters could have a large effect on the speed and degree of swelling during recovery mode. For example, if a buffer solution as is commonly used in LOC applications is employed, the results could differ from those obtained using pure water. This requires further study.

Also requiring further study is the reliability of the microvalves. Although the microvalves were tested over multiple cycles, they were not tested for failure modes. Furthermore, while no obvious difference in operation was noticed over five to ten cycles, variation in performance over time should be characterized.

In addition, potential application such as tissue engineering, controlled drug delivery for such flexible microvalve needs to further researched towards a fully developed and practical device. An arm patch drug delivery is also probable due to the operation temperature of 32-34°C(closer to body temperature).

APPENDICES

APPENDIX A: List of Publications

1.A.Li, J.Lee, B.G. Gray, Paul C.H.Li, "Fabrication and testing of the hydrogel-based microvalves for flow control in flexible lab-on-a-chip systems" , *SPIE Proc*, Vol.8251-35, 2012

2.A.Li, A.Khosla, C.Drewbrook, B.G. Gray, "Fabrication and Testing of the hydrogel-based actuators using polymer heater elements for flexible microvalves", *SPIE Proc*, Vol.7929-13, 2011.

3.A.Li, A.Khosla, B.Gray, J.Lee, Paul Li, "Fabrication and testing of the hydrogel-based microvalves for lab-on-a-chip application" Lab on a chip World Congress, poster, San Francisco, 09-122011.

4. A.Li, B.G Gray, "Hydrogel-based microvalve simulation" COMSOL Multiphyiscs Conference Boston 2011, Boston MA

5. C.Drewbrook, A.Khosla, Ang Li, "Fabrication and testing of Tungsten nanoparticles doped polymer for lab-on-a-chip application" , CMBEC 2010, Vancouver, BC

6.A. Li, B.G Gray, "XXXXXXXX" to be submitted to Journal of Micromechanics and Microengineering

APPENDIX B:DETAILED FABRICATION PROCESS

For the devices described in section 4, this section lists the detailed steps for the fabrication processes. My process is listed in Table B-1.

Table B-0-1: Photolithography process for making microheater on glass substrate/ pyrex wafer

First of all, Clean glass slides were cleaned with Acetone, IPA and DI water.

Processing steps	Details
Sputtering	100 nm of Gold, 10 nm of Chrome.
Spincoat SU-8	S1813 PR, 3 full droppers, makes sure PR spread evenly. Spin at 4000 RPM for 30s.
Softbake	Baked on hotplate from 110ºC to 120ºC for 2 minutes
Align and expose	No optical filter needed, UV exposure of 365 nm for 60s
Post-exposure bake	Post-exposure bake should take place directly immediately after exposing
Development	Slight agitation, the development times depended on the structure needed
Rinse and Dry	Spray/wash with Isopropyl Alcohol(IPA) for 10 seconds

Please noted In some work, there was clear indication that the prebake, exposure, and development time had the largest affect on the aspect ratio of the fabricated structures.

Table B-0-2: Photolithography process for ~ 100 µm thick SU-8 2035 master mold

Processing Step	**Details**
Substrate Pretreat	RCA clean using DI H_20:NH_40H:H_2O_2 (5:1:1) at 80°C for 10 min. then rinses with acetone, IPA, then water (3 times each slide). After the cleaning, blow dry and perform a (~10 min) dehydration bake in the small ovens.
Spin SU-8	Pour SU8-2035 carefully and evenly (Dispense 1ml of resist of each inch of substrate). Spin at 1200 RPM for 30 seconds
Softbake	Baked on hotplate from 35°C to 95°C for 20 minutes, with ramping 450°C/hr. Cool down for 10 minutes
Align and expose	UV exposure of 365 nm for 120 seconds, (exposure energy 230mJ/cm^2 x 1.5x=345mJ)
Post-exposure Bake	PEB should take place directly after exposure time. PEB at 95°C for 15 minutes.
Develop	Gently agitation in SU-8 Developer for 10 minutes
Hard bake	120°C for 20 minutes(optional)

PDMS structures on SU-8 molds were fabricated as listed in Table B-3.

Table B-0-3 : Fabrication process for PDMS using SU-8 2035 molds

Step	**Details**
Make SU-8 mold	Table B-2.
Mix and degas PDMS	Use the spoon to dispense the PDMS base and curing agent(in 10:1 ratio, 10 parts of elastomer and 1 part of curing agent) Weigh the PDMS pre-polymer components in 10:1(base: curing agent) ratio in the cup. Add the base first, Mix well with the stirring rod.
Pour PDMS	Carefully pour the PDMS over the SU-8 master located in the petri dish
Vacuum in mold	Vacuum out bubbles due to pouring in mold, for 10-30 minutes, until most visible bubble are removed
Cure PDMS	Place the sample on the hotplate. Set the hotplate to 60 °C.
Remove mold	Using tweezers, carefully peel off the PDMS mold from the SU-8 master

APPENDIX C:MASK DESIGNS

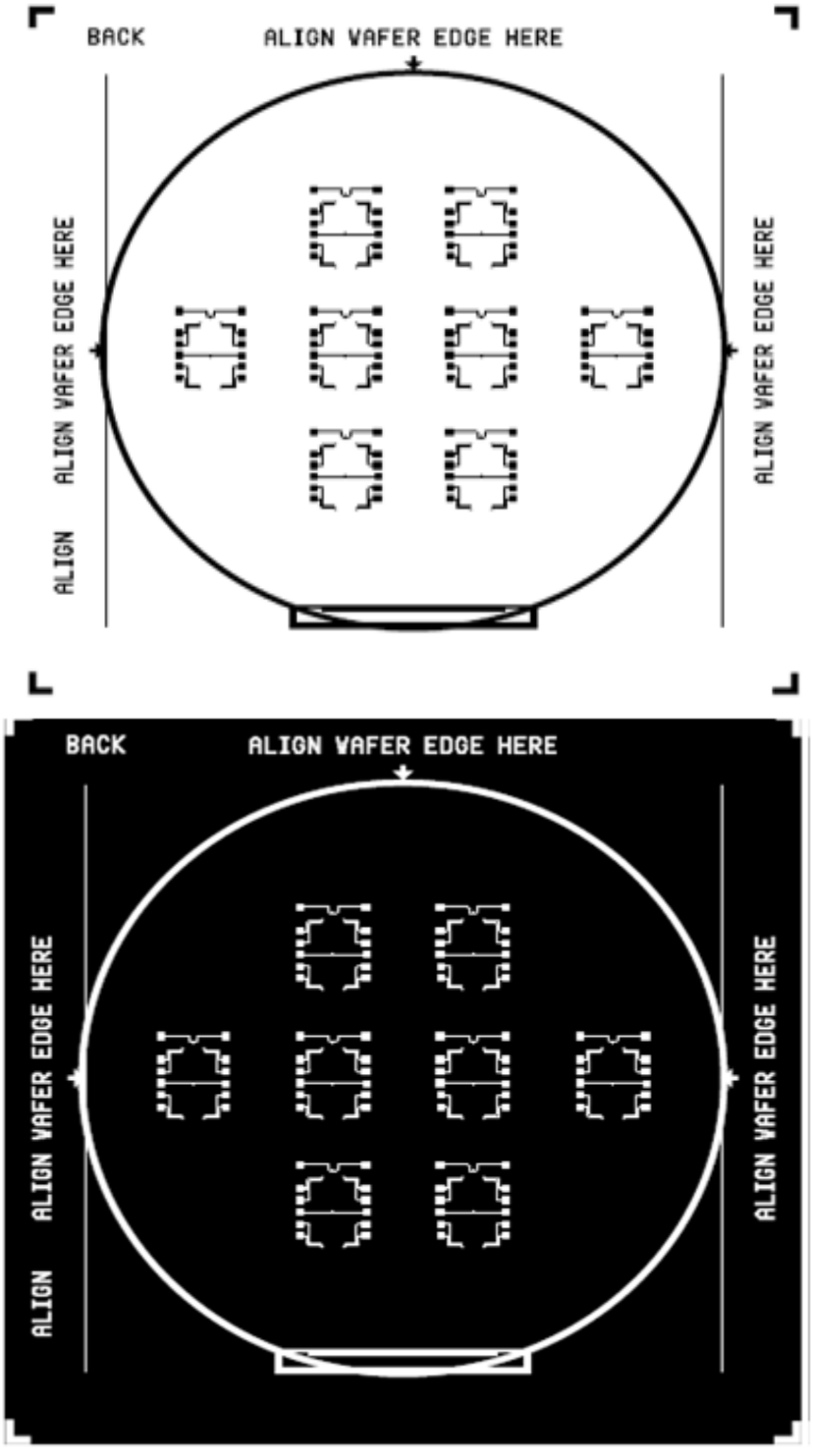

Figure C-1 Mask Layout for Flexible microheaters (a)Positive (b)Negative)

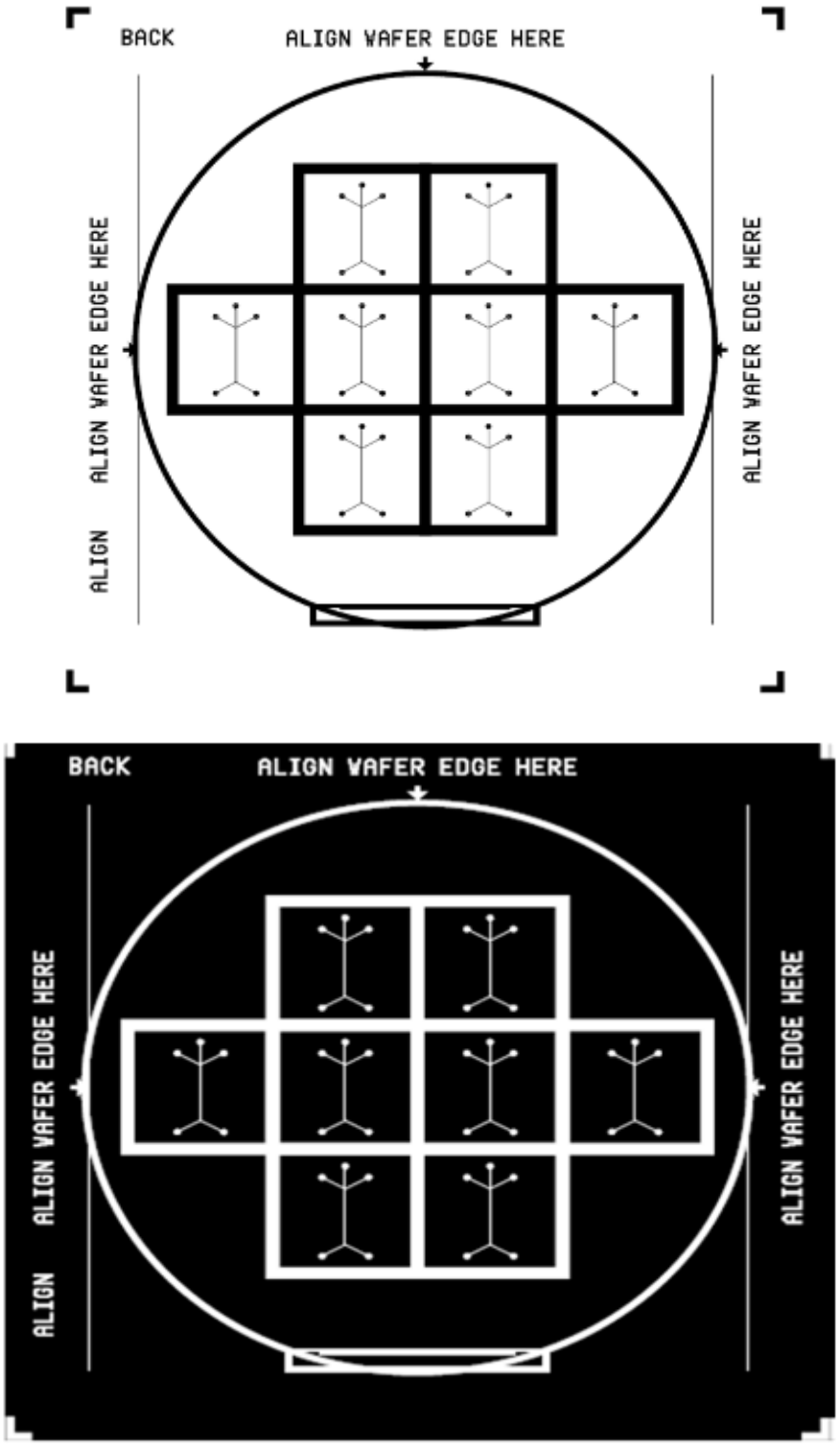

Figure C-2. Mask layout for PDMS Microchannel(a) Positive (b) Negative

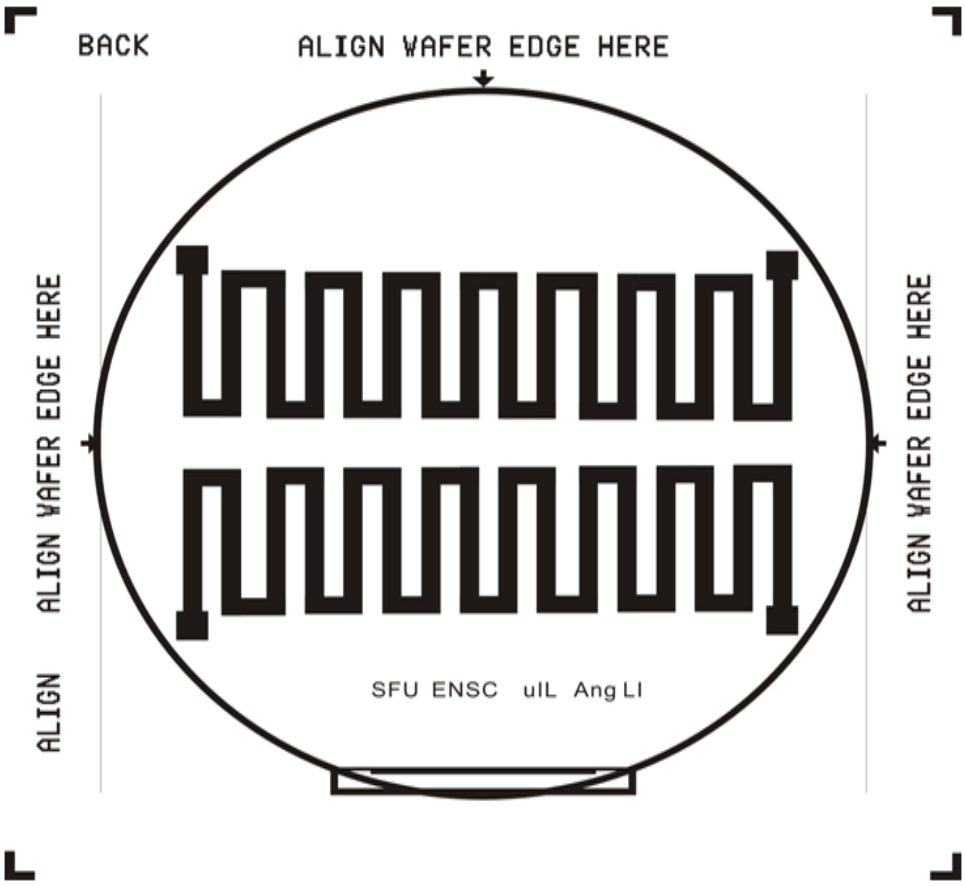

Figure C-3 Mask Layout for Carbon Nanotubes heaters(CNT) heaters

APPENDIX D: Hydrogels Scanning Electron Microscope Procedure

D1. Hydrogel Freeze Drying Procedure

1. Freezing

The hydrogel samples were placed in the flask in the liquid nitrogen bath as illustrated in Figure D-1. Usually, the freezing temperature are between -50°C and -80°C. The freezing phase is the most critical in the whole freeze-drying process. It is important to cool the material to its triple point. This step is to ensure the sublimation of the sample instead of vaporization.

Figure D1. Optical images of the hydrogels sample placed in liquid nitrogen(N_2) bath with temperature below zero.

2. Drying

During the primary drying phase, the pressure is lowered, and enough heat is supplied to the material for the water to sublime. As illustrated in Figure D-2, a freeze drying flask was mounted on the freeze dryer. It aims to remove unfrozen water molecules. This entire process took more than 12 hours(overnight).

Figure D-2 The freeze-drying flask mounted on the lyophilizer

D2. Hydrogel Gold Sputtering Procedure(Performed in the Nano-imainging facility)

Au- Sputtering Procedure(Field Emission Scanning Electron Scope of the Hydrogel)

1. Pre-sputtering check
a. Ar pressure at 6psi.
b. Au source and related tool are avaiable.
c. Samples are ready.
d. Main power off.
e. Take the glass cylinder chamber off and put in a safe place.
f. Install Au sputter source to the top plate.
g. Put samples and thickness monitor on the stage.
h. Install the glass chamber and lower top plate.
i. Main power off

2. Set Operatical controls

Control	set to
Main Power Switch	off
Voltage Switch	off
Voltage Control	0
Gas on/off switch	off
Reset/Auto Switch	Middle position(Default)
Pulse	off
Mode switch	Plate

3. Start work
a. Main power on.

Place your hand on the top of the chamber to secure pumping down at the very beginning until the meter reading counts down.
b. Gas on/off switch on.
c. Flush chamber with Ar gas: Rotating the gas control knob counter clockwise slowly till vacuum displaying 180 millitorr.
Turn the Gas on/off switch off. Allow the vacuum to reach 30 millitorr. Repeat the process b
& c 2 more times.

d. Stabilize vacuum at 40 to 60 millitorr.
e. voltage switch on.
f. Adjust gas control and voltage control for stable conditions of 15 milliamps at 60 to 80 millitorr.
g. For pulse operation: set Pulse switch on.
h. Set sputtering time, ref. to the diagram.
i. Reset/Auto switch to auto.
j. When desired sputtering time has been reached, turn to shut down procedure.

4. Shut down procedure

a. Voltage control to zero
b. voltage switch off
c. Gas on/off switch off
d. Reset/Auto Switch to middle position(Default)
e. Pulse Switch
f. Main power switch off
g. Allow system to vent to atmosphere
h. Take the glass cylinder chamber off and put in a safe place!
i. Remove the samples
j. Take off Au source with related tool

APPENDIX E: Equipment List

E.1 SFU Engineering Science Microinstrumentation Laboratory

1. Digital Multimeter: Fluke 8010A
2. Syringe pump: Harvard Apparatus
3. Camera: Canon Powershot S3-IS
4. Microscope: Motic SMZ-168
5. Micromanipulator: Model # PR0198 wentworth laboratory
6. Hot plate: Fisher Thermix Model 210

E.2 SFU Engineering Science Cleanroom

1. Photoresist Spinner: Headway research
2. Mask Aligner: Quintel Q-2001CT
3. Hot plates: Torrey Pines Scientic Ecotherm-TM Digital Hot plate
4. Reactive Ion Etch(RIE): Benchmark 800

E.3 SFU Surrey Machine Shop

1. Laser cutter: Universal Laser Systems VLS 3.60 CO_2 Laser

2. Corel Draw X4

E.4 SFU Department of Chemistry

1. Nitrogen Tank
2. Bio-safety cabinet
3. SFU Chemical storage room
4. Liquid Nitrogen
5. Freeze Dryer(Lyophilizer)

E5. SFU Nanoimaging Facility

1. Strata DB235 FESEM/FIB

2. Baush & Lomb Nanolab SEM

3. Au Sputter Coater

4. Cryo SEM

5. Hitachi 8000 STEM

6. Energy Dispersive X-ray(EDX) Instrument

References List

[1] D. J.Beebe, J. S. Moore, J. M. Bauer, Q. Yu, R. H. Liu, C. Devadoss, B-H. Jo, " Functional structures for autonomous flow control inside micro fluidic channels," *Nature*, vol. 404, pp. 588-590, 2000.

[2] E.T., Lagally, J.R Scherer., R.G Blazej., N.M., Toriello B.A ,Ramchandani, M., Sensabaugh G.F., L.W.Riley, and R.A. Mathies, "Integrated Portable Genetic Analysis Microsystem for Pathogen/Infectious disease detection"

[3] K..W.Oh , and C.H,Ahn, "A review of microvalve," *Journal of Micromechanics and Microengineering*, 16, R13-R39, 2006

[4] M.Tabib-Azar, "Microactuators: "*Electrical, Magnetic, Thermal, Optical, Mechanical, Chemical, and Smart Structures*", Norwell MA: Kluwer Academic ,1998

[5] C. Fu, Z. Rummler, and Schommburg, " Magnetically driven micro ball valves fabricated by multilayer adhesive film bonding," *Journal of Micromechanics and microengineering*, 13, S96,2003

[6] M Shikida,,K Sato, S.Tanaka , Y. kawamura., and Y.Fujisaki., "electrostatically driven gas vlave with high conductance," Journal of Microelectromechanical Systems 3, 76 ,1994

[7] S.Kluge, G Klink, and P Woias, "A fast switching, low power pneumatic micro- valve made by silicon micromachining", *American Laboratory* 30, 17 ,1998

[8] I. Chakraborty, W.C, Tang, and T.K. Tang, "MEMS micro-valve for

space applications," *Sensors and Actuators a-Physical* 83, 188 ,2000

[9] B .Becker, W.J.Wang, "Microfluidics, BioMEMS, and Medical Microsystems VIII" , *SPIE Proceeding*, 2010.

[10] S .Coyle, Lau, K.T, Moyna.N, O'Gorman and Diamond,D, "BIOTEX—Biosensing Textiles for Personalised Healthcare Management", *IEEE Transactions on Information Technology in Biomedicine* 14(2):364-370 ,2010.

[11] J.N.,Patel, B.L.,Gray, ,B.Kaminska, B.D Gates, "Flexible glucose sensor utilizing multilayer PDMS process", *IEEE 30th Annual Eng in Med & Biology Conf*, Vancouver, 4 pp, 2008.

[12] C. Yu, S. Mutlu, P .Selvaganapathy, C.H Mastrangelo, F .Svec and Fre´chet JMJ (2003a)"Flow control valves for analytical microfluidic chips without mechanical parts based on thermally responsive monolithic polymers,", *Anal Chem* 75:1958–1961.

[13] R.H , Liu, Q Yu, and Beebe, D., "Fabrication and characterization of hydrogel-based microvalves", *Journal of Microelectromechanical Systems*, 11(1), 45-53 ,2002.

[14] B.Stoeber, D Liepmann, Muller,S.J, "microvalve concepts based on thermally-responsive triblock copolymers', P*roceedings of the XIVth International Congress on Rheology*, Seoul, Korea,2004.

[15] R.H Liu, Q. Yu,. and D. Beebe, "Fabrication and characterization of hydrogel-based microvalves", *Journal of Microelectromechanical Systems*, 11(1), 45-53 ,2002.

[16] C .Fu, Z .Rummler,., and Schommburg, " Magnetically driven micro ball valves fabricated by multilayer adhesive film bonding," *Journal of Micromechanics and microengineering*,13, S96,2003.

[17] M .Shikida, K .Sato, S Tanaka, Y. kawamura, and Y.Fujisaki., "electrostatically

driven gas vlave with high conductance," *Journal of Microelectromechanical Systems* ,3, 76 ,1994

[18] S.Kluge, Klink,G, and Woias,P, "A fast switching, low power pneumatic micro- valve made by silicon micromachining", *American Laboratory*, 30, 17 ,1998

[19] C .Yu, S .Mutlu, P .Selvaganapathy, CH . Mastrangelo, Svec F, Fre´chet JMJ (2003a)"Flow control valves for analytical microfluidic chips without mechanical parts based on thermally responsive monolithic polymers,", *Analytical Chemistry* ,8,1961.

[20] G.Gerlach, K.F Arndt, *Hydrogel sensors and actuators* ,Springer, London& New York,205-225,2009

[21] G .Chen, F Svec, D.R.Knapp, "Light-actuated high pressure-resisting microvalve for on-chip flow control based on thermo-responsive nanostructured polymer" *Lab on a Chip*,8:1198–1204,2008

[22] A.Richter, D.Kuckling, S .Howitz, T .Gehring, and K.F .Arndt, "Electronically controllable microvalves based on smart hydrogels: magnitudes and potential applications.", *J Microelectromech Syst* 12:748–753,2003.

[23] J.Wang, Z.Chen, M.Mauk, K.S.Hong, M.Li, S.Yang, and H.H.Bau, "Self-actuated, thermo-responsive, hydrogel valves for lab on a chip,"*biomedical microdevices*,313-325,2005

[24] A .Richter, KF .Arndt, W .Krause, D. Kuckling, S .Howitz, "Devices for flow control based on smart hydrogels," *7th Pacific polymer Conference*, Oaxaca, Dec 3–7, p. 31,2001.

[25] C,Yu , S .Mutlu, P. Selvaganapathy, C.H. Mastrangelo, F. Svec, Fre´chet JMJ " Flow control valves for analytical microfluidic chips without mechanical parts based on thermally responsive monolithic polymers" *Analtical Chemistry*,75(8),

2003.

[26] Q. Luo, S.Mutlu, YB. Gianchandani, F. Svec, Fre´chet JMJ Monolithic valves for microfluidic chips based on thermoresponsive polymer gels. *Electrophoresis* 24:3694–3702, 2003

[27] S.Sugiura, K .Sumaru, K .Ohi, K .Hiroki, T. Takagi, T. Kanamori Photoresponsive polymer gel microvalves controlled by local light irradiation. *Sensors and Actuators A* 140:176–184, 2007

[28] G .Chen, F .Svec, DR .Knapp" Light-actuated high pressure-resisting microvalve for on-chip flow control based on thermo-responsive nanostructure polymer," *lab on a chip*,8,1198-1204, 2008.

[29] A .Richter, C .Klenke, Arndt KF, "Adjustable low dynamic pumps based on hydrogels, *"Macromolecule Symposium*, 210:377–384, 2004.

[30] B.T,.Good, C.N Bowman, R.H Davis. "A water-activated pump for portable microfluidic applications," *J Colloid Interface Sci*,305:239–249,2007

[31] DJ. Beebe , JS Moore, J.M ,Bauer, Q .Yu, RH .Liu, C. Devadoss ,JO, BH "Functional hydrogel structures for autonomous flow control inside microfluidic channels," *Nature* ,404:588,2000.

[32] A .Baldi, Gu Y, PE .Loftness, RA .Siegel, B. Ziaie "A hydrogel-actuated environmentally sensitive microvalve for active flow control," *Journal of Microelectromechanical System* ,12:613–621,2003.

[33] N.Alavi" Microchannel Fabrication from PMMA by CO2 Laser Laboraotry Manual", *SFU Co-op report*,2009.

[34] http://www.nanotech.dtu.dk/Research/Research%20groups/Nanoprobes/Research/General%20Activities/Polymeric%20sensors/Material.aspx,2011

[35] E.H .Schacht,., "Polymer chemistry and hydrogel systems", *Journal of Physics: Conference Series* **,3** 22–2,2004

[36] Y.X .Wang, X.F Wang, S.W Song, " Synthesis, characterization and controlled

drug release of thermosensitive Poly(NIPAAm-co-HEMA), "*Advanced Materials Research*, 11-12, 737,2006

[37] H.Omidian, J.G. Rocca, and K. Park,., "Advances in superporous hydrogels", *Journal of controlled release*,2005

[38] R.A Gemeinhart, H Park, and K. Park, "Pore structure of superporous hydrogels, "*Polymers for advanced technologies*,11,617-625,2000

[39] C .Drewbrook, A.Khosla, A. Li, "Fabrication and testing of tungsten nanoparticle doped polymer microheaters for lab on a chip application" *Proc.33rd CMBEC*, Vancouver, BC, Canada,2010

[40] A. Richard, Gemeinhart, "pH sensitive of fast response superporous hydrogels" *Journal of Biomater Sci. Polymer* Edn, Vol.11,2000

[41] http://chemistry.about.com/od/factsstructures/ig/Chemical-Structures---A/Acrylamide.htm, 2011.

[42] A.Li,A.Khosla,C.Drewbrook,B.G. Gray, "Fabrication and Testing of the hydrogel-based actuators using polymer heater elements for flexible microvalves", *SPIE Proc*, Vol.7929-13, 2011.

[43] COMSOL® Inc , "MEMS Module User guide(version 4.1)", COMSOL®, Inc, 2009.

[44] N.T Nguyen and S.T .Wereley, *Fundamental and applications of microfluidics*, Artech house, Boston& London, 2006.

[45] D. T. Eddington and D. J. Beebe, ‘‘Flow control with hydrogels, "Flow control with hydrogels’’, *Advanced Drug Delivery Review*, , 56,199–210, 2004

[46] X. Cao, S. Lai and L. J. Lee, ‘‘Design of a self-regulated drug delivery device’’, *Biomedical Microdevices*, 3, 109–118,2001.

[47] http://drugdelivery.chbe.gatech.edu/research.html,2006.

[48] Sudipto K De, N.R.Aluru, B Johnson, W C Crone, DJ Beebe, J.Moore

"Equilibrium Swelling and kinetics of pH-Responsive Hydroges: Models, Experiments, and Simulations", *Journal of Microelectromechanical systems*, vol.11, 5, 2002.

[49] I.Tokarev, S.Minko, "Stimuli-responsive thin films", *soft matter*, 5,511-524, 2009.

[50] T.Xu, J.M.Miao, H.Li, Z.H. Wang"Local synthesis of aligned carbon nanotube bundle arrays by using integrated micro-heaters for interconnect applications", 20, *Nanotechnology*, 2009

[51] K. Haubert, T.Drier, D. Beebe, "PDMS Bonding by means of portable, low-cost corona system", *Lab on a chip*, 6, 1548-1549, 2006

[52] M. Potter, D.C Wigghert, *Fluid Mechanics*,New York, Mcgraw-Hill, 2008.